Geodynamic implications of paleomagnetic data from Tertiary sediments in Sakhalin, Russia (NW Pacific)

Richard Weaver and Andrew P. Roberts

School of Ocean and Earth Science, University of Southampton, Southampton Oceanography Centre, Southampton, UK

Rachel Flecker[1] and David I. M. Macdonald[2]

Cambridge Arctic Shelf Programme, Department of Earth Sciences, University of Cambridge, Cambridge, UK

Lidiya M. Fot'yanova

Paleontological Institute, Russian Academy of Sciences, Moscow, Russia

[1]   N-S trending right-lateral strike-slip faults, which were active in the Tertiary, transect Sakhalin, Russia, while Mesozoic forearc and accretionary rocks testify to an earlier period of subduction. Several kinematic models have been proposed for the region, but the details required to constrain these models, such as the timing of the transition from subduction to strike-slip tectonics in Sakhalin, are still unknown. Even first-order tectonic features, such as the boundaries of the plates with which Sakhalin evolved during the Tertiary, are poorly known. Paleomagnetic results from around Sakhalin were obtained to constrain the geodynamic evolution of the region. Comparison of paleomagnetic inclination data with the apparent polar wander paths for the Eurasian, Pacific, and North American Plates suggests that Sakhalin probably evolved with the North American Plate, although a history including the Eurasian Plate cannot be ruled out. Paleomagnetic declination data suggest that significant clockwise vertical axis rotation has occurred in Sakhalin since the mid-Paleocene. It is likely that this rotational deformation was accommodated by Tertiary activity on right-lateral strike-slip faults, which may be associated with the opening of the Japan Sea, Tatar Strait, and Kuril Basin. These data contradict a published kinematic model for eastern Sakhalin, where counterclockwise vertical axis rotations were predicted for Neogene basins in the East Sakhalin Mountains. Agreement is better, however, with published paleomagnetic data from southern Sakhalin, where clockwise vertical axis rotations were documented.   *INDEX TERMS:* 1525 Geomagnetism and Paleomagnetism: Paleomagnetism applied to tectonics (regional, global); 3040 Marine Geology and Geophysics: Plate tectonics (8150, 8155, 8157, 8158); 8150 Tectonophysics: Evolution of the Earth: Plate boundary—general (3040); 9320 Information Related to Geographic Region: Asia; 9604 Information Related to Geologic Time: Cenozoic; *KEYWORDS:* Paleomagnetism, Sakhalin, plate tectonics, Okhotsk Sea, Asia, Cenozoic

1.   Introduction

[2]   The plate configuration of the NW Pacific margin, around the Okhotsk Sea, is complex and the positions of boundaries between the Pacific, North American, Eurasian and Okhotsk Sea plates have not been precisely determined. This is partly due to the sparse distribution of seismic events, particularly in the NE part of the Asian continent [*Riegel et al.*, 1993; *Seno et al.*, 1996]. A wide zone of N-S trending strike-slip faults, which crops out on Sakhalin, is considered to represent an active transform plate boundary, but it is uncertain which plates are interacting in this area (Figures 1 and 2) [*Seno et al.*, 1996]. The Tertiary geodynamic evolution of Sakhalin is also unclear. A Mesozoic accretionary complex in Sakhalin indicates a previous period of subduction (Figure 1c), but a transition to a dextral transpressive regime occurred some time in the Tertiary [*Kimura*, 1994]. Deep-sea drilling in the Okhotsk Sea could reveal vital geological data, particularly regarding

---

[1]Now at School of Geographical Sciences, University of Bristol, Bristol, UK.

[2]Now at Department of Geology and Petroleum Geology, University of Aberdeen, Aberdeen, UK.
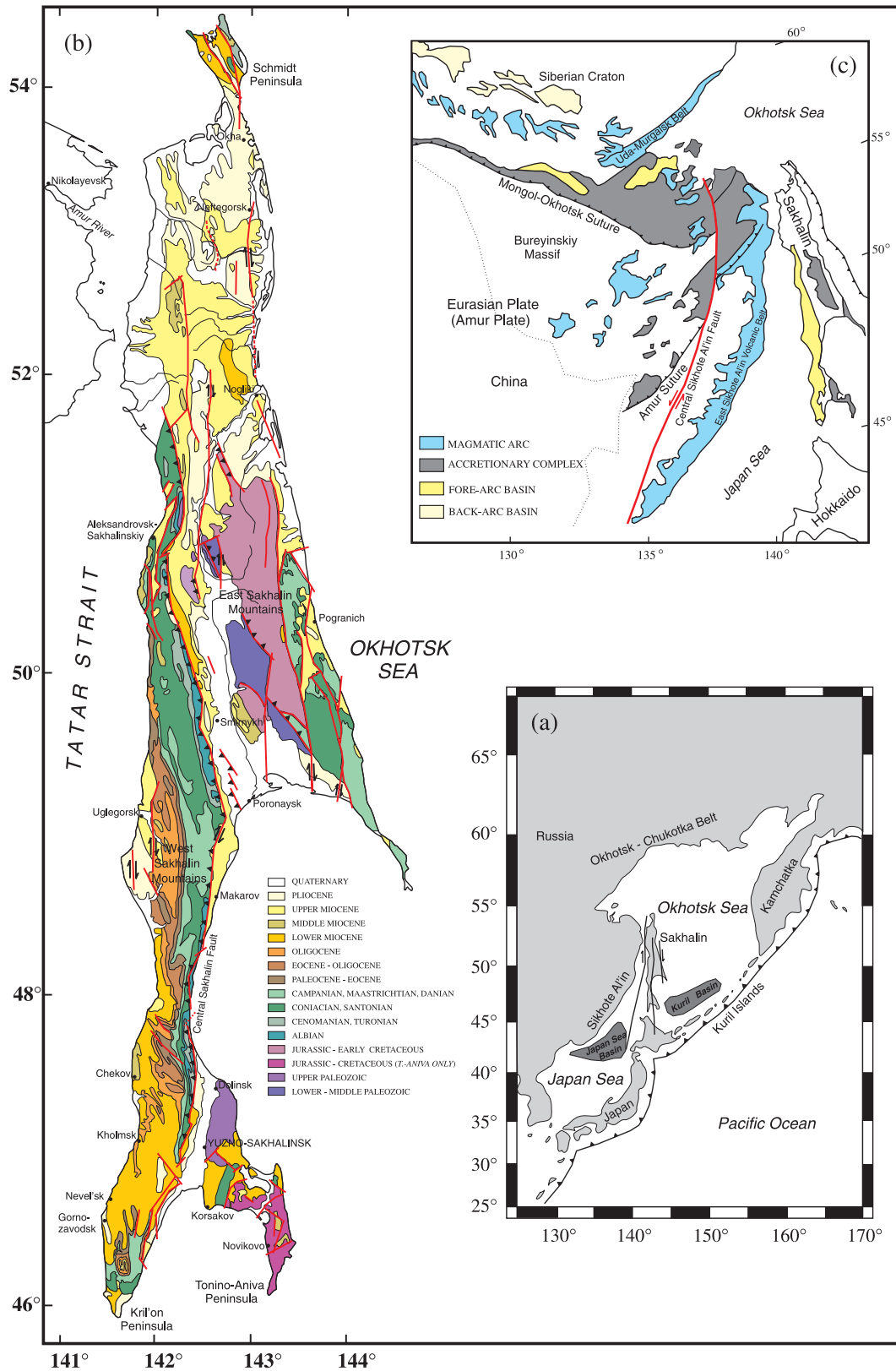
Figure 1. (a) Sketch map of the Okhotsk Sea region showing the N-S trending faults across Sakhalin. Darker shading indicates the location of proven or postulated oceanic crust. Modified after *Seno et al.* [1996]. (b) Geological map of Sakhalin. Compiled from various sources [*Vereshchagin*, 1969; *Rozhdestvenskiy*, 1982; *Kharakhinov et al.*, 1985; *Fournier et al.*, 1994; *Ivashchenko et al.*, 1997]. (c) Map of major suture zones and tectonostratigraphic units in southeastern Russia. Modified after *Natal'in* [1993].
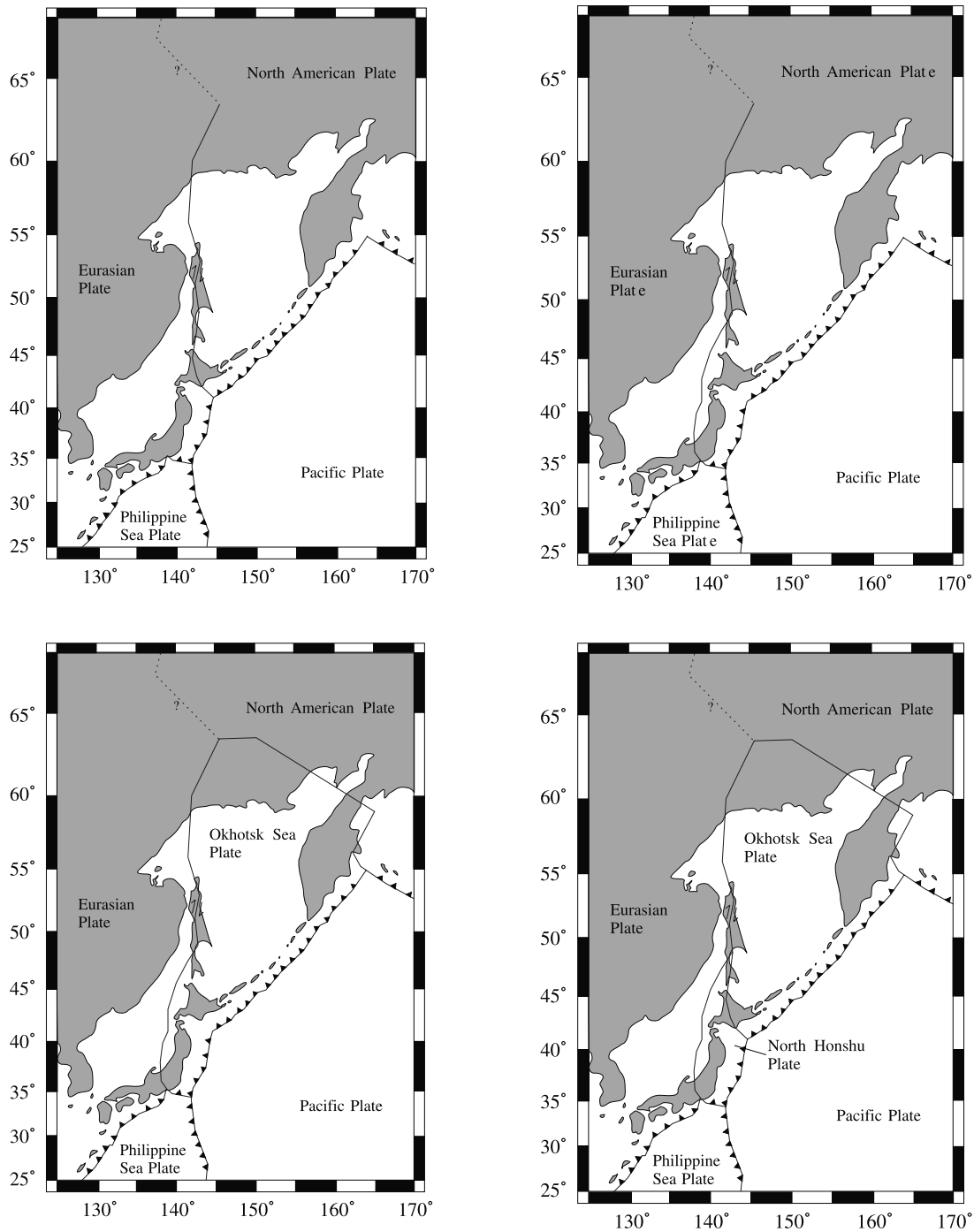
Figure 2. Possible plate configurations in NE Asia [after *Seno et al.*, 1996].

the age of sedimentary basins, but this has not been carried out. In this study, we use paleomagnetic methods to address these first-order tectonic issues, and to develop an improved understanding of local tectonics. Paleomagnetic methods have proved valuable for constraining the geodynamic evolution of tectonically complex regions, such as the Philippines [*Fuller et al.*, 1989], the Aegean Sea [*Kissel and Laj*, 1988], New Zealand [*Little and Roberts*, 1997] and California [*Luyendyk et al.*, 1985]. Paleomagnetic work has been previously carried out on Tertiary rocks from three localities in southern Sakhalin [*Takeuchi et al.*, 1999], but

no other paleomagnetic work has been reported on the Tertiary evolution of Sakhalin.

[3] Several kinematic models for the NE Asian margin have been proposed which include Sakhalin and the Okhotsk Sea and suggest strike-slip deformation, pull-apart basin formation and vertical axis rotations of crustal-scale blocks [e.g., *Jolivet et al.*, 1995; *Worrall et al.*, 1996; *Takeuchi et al.*, 1999]. Many of the data on which these models are based are from Japan and the Japan Sea, and it is not clear how Sakhalin has deformed. There are two models that suggest rotation of fault-bounded "domino" blocks in Sakhalin
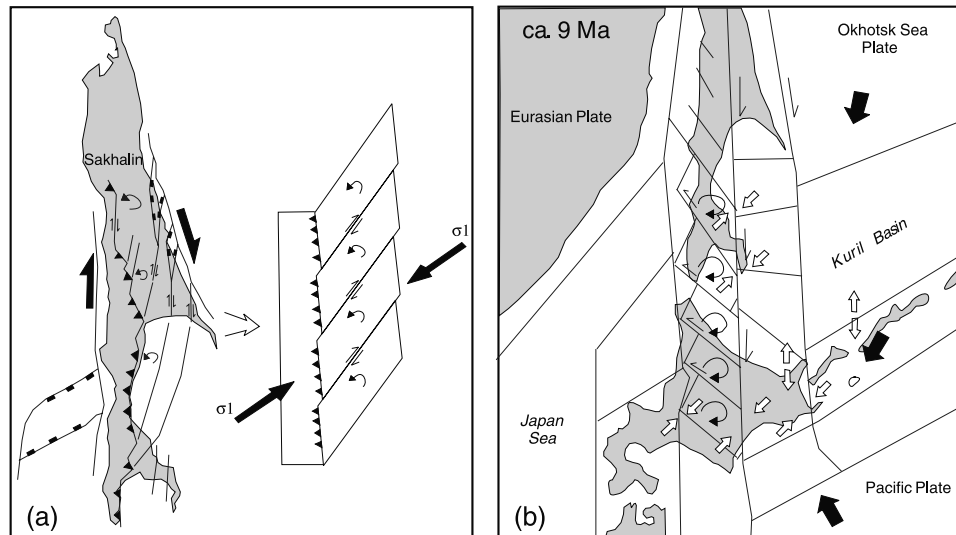
Figure 3. (a) Tectonic model for vertical axis rotations in Sakhalin, as proposed by *Fournier et al.* [1994], showing counterclockwise block rotation during Neogene basin formation in eastern Sakhalin. (b) Tectonic model for vertical axis rotations in Sakhalin and Hokkaido, as proposed by *Takeuchi et al.* [1999], showing clockwise block rotation during opening of the Japan Sea. The rotational mechanism has been linked to the synchronous opening of the Kuril Basin.

(Figure 3). *Fournier et al.* [1994] suggested that counterclockwise rotations would be expected for Neogene basins in eastern areas of Sakhalin (Figure 3a). More recent work by *Takeuchi et al.* [1999], based on paleomagnetic data from Hokkaido and southern Sakhalin, suggests that clockwise rotations have occurred, accommodated by 100-km-scale crustal blocks, which are part of a domino system that could extend southward to Hokkaido, Japan (Figure 3b). However, there are several problems with domino models. What happens at the edges of crustal blocks? With the fault geometries indicated in such models, triangular zones of compression or extension would be expected at the boundaries of the blocks [e.g., *Luyendyk et al.*, 1980; *Hornafius et al.*, 1986; *Roberts*, 1995; *Townsend and Little*, 1998; *Bayasgalan et al.*, 1999]. These structures are not evident in the field in Sakhalin. Also, rotations of more than 25° are theoretically impossible on a single set of planar faults [e.g., *Nur et al.*, 1989]. Evidence for multiple fault sets should therefore be expected to accommodate large-scale rotations.

[4] Paleomagnetic data presented here should allow more accurate identification of rotated domains in Sakhalin, and may justify reconsideration of the existing kinematic models for evolution of the NE Asian margin. In this study, we aim to address the following questions. (1) With which plates has Sakhalin interacted and evolved? (2) When did the transition from subduction to strike-slip tectonics occur in Sakhalin? (3) By which structural mechanisms did the transition occur?

2. Geological Background and Sampling

2.1. Regional Geology

[5] Sakhalin comprises two main tectonic zones separated by the N-S trending Central Sakhalin Fault (Figure 1b). To the east, Mesozoic accretionary complex material has been uplifted [e.g., *Rikhter*, 1984; *Parfenov and Natal'in*, 1986].

These blueshist and greenshist facies metamorphic rocks are exposed in the East Sakhalin Mountains, NE Schmidt Peninsula, and on the Tonino-Aniva Peninsula in southern Sakhalin [*Vereshchagin*, 1969] (Figures 1b and 1c). Small Tertiary depocenters, which may have pull-apart origins, also exist in these areas [*Worrall et al.*, 1996]. West of the Central Sakhalin Fault, there is a thick sequence of Mesozoic forearc sediments [*Parfenov and Natal'in*, 1986; *Zyabrev and Bragin*, 1987] (Figures 1b and 1c). The corresponding Mesozoic-Cenozoic volcanic arc is the East Sikhote Al'in Volcanic Belt [*Zonenshain et al.*, 1990; *Okamura et al.*, 1998] on the Russian mainland (Figure 1c).

[6] Northeastern Russia is made up of a series of accreted terranes. Crustal blocks are defined and separated by magmatic arcs and accretionary complexes; arcs also stitch across earlier sutures [*Natal'in*, 1993]. The Mongol-Okhotsk Suture, which stretches from the northern side of the Sea of Okhotsk to SE Siberia, marks the Permian to Jurassic northeastward oblique collision of the Bureyinskiy Massif with the Siberian Craton (Figure 1c). A second suture, the Amur Suture, formed to the west of Sikhote Al'in in the Cretaceous by subsequent accretion of the Sikhote Al'in terrane. During accretion of Sikhote Al'in, subduction on the east side of the Russian mainland created the Late Cretaceous-Paleogene Sikhote Al'in volcanic arc. *Zonenshain et al.* [1990] suggested that oceanic subduction also occurred farther east to give rise to the "East Sakhalin Arc." The unknown oceanic plate separating the "East Sakhalin Arc" from Sikhote Al'in was consumed through westward subduction. Late Cretaceous-early Eocene volcanic rocks in Sikhote Al'in are usually assumed to be associated with this subduction event and are the source of forearc sediments in west Sakhalin [*Zonenshain et al.*, 1990].

[7] Paleocene to Pliocene sediments were targeted for this paleomagnetic study (Figure 4). These sedimentary rocks occur in a variety of settings, including (1) Tertiary terres-
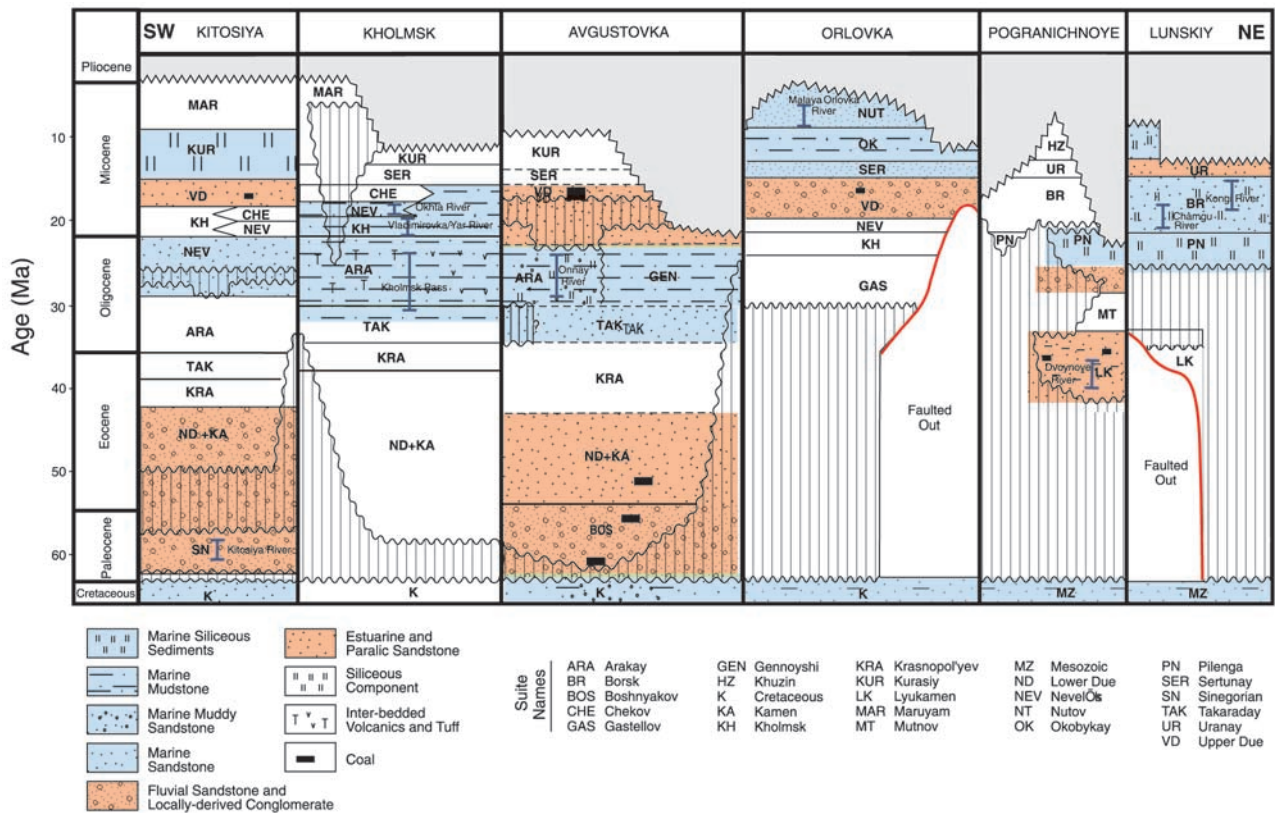
Figure 4. Stratigraphic sections of Sakhalin. Paleomagnetic sampling sites are indicated by vertical bars with names of the sampled localities. Only the samples taken from marine successions have well-constrained ages. The ages of paralic and continental sediments are subject to much greater errors. The stratigraphic information is derived from *Vereshchagin* [1969], *Gladenkov* [1988], *Menner et al.* [1977], *Serova and Fot'yanova* [1981], *Zhidkova and Sal'nikov* [1992], and *Fot'yanova et al.* [2001].

trial sequences, which mostly lie to the west of the West Sakhalin Mountains and date back as far as the Paleocene, (2) marine and continental sediments in the central valley and in small basins peripheral to the East Sakhalin Mountains; these are mostly of Oligocene and younger age, and (3) lower Miocene-Pliocene sediments of the Amur delta in central northern areas (Figures 1b and 1c). Late Mesozoic and late Cenozoic tectonic events have strongly deformed sediments in the West Sakhalin Mountains [*Vereshchagin*, 1969] with NW-SE trending mesoscale folds associated with late Cenozoic faulting [*Rozhdestvenskiy*, 1982; *Fournier et al.*, 1994].

2.2. Field Sampling

[8] Dating and correlation of the Cenozoic sediments on Sakhalin are hampered by the predominance of continental and paralic strata. A relatively good lithostratigraphic framework has been constructed, constrained in part by biostratigraphic data from the successions deposited during episodic marine transgressions [*Menner et al.*, 1977; *Serova and Fot'yanova*, 1981; *Gladenkov*, 1988; *Zhidkova and Sal'nikov*, 1992; *Fot'yanova et al.*, 2001]. Recent isotopic dating of Tertiary volcanic rocks on Sakhalin [*Takeuchi*, 1997; *Okamura et al.*, 1998] broadly supports this framework, but the general accuracy of the chronostratigraphy, particularly in the continental parts of the succession, is difficult to judge.

[9] The approximate stratigraphic range of paleomagnetic samples is indicated by vertical bars on the stratigraphic columns in Figure 4. Approximately 40 samples were taken from throughout the stratigraphic sequence at each locality in order to obtain a mean paleomagnetic direction for which the geomagnetic secular variation has been adequately averaged. Paleomagnetic samples were collected from a diverse suite of Cenozoic rocks with a wide geographic distribution: southwest of the region dominated by strike-slip faulting, local to the Central Sakhalin Fault, and in the far east of Sakhalin (Figures 4 and 5). A total of 1574 samples was collected from 28 localities around Sakhalin (Figure 5 and Table 1). However, only nine localities (160 samples) yielded reliable paleomagnetic data (Figure 5 and Tables 1 and 2); samples from 12 localities were remagnetized, and samples from the other seven localities were too weakly magnetized to provide reliable paleomagnetic data. The localities that yielded reliable paleomagnetic results are listed in Table 1, which includes details of the local stratigraphy and structure.

3. Methods

3.1. Paleomagnetic Measurements

[10] The natural remanent magnetization (NRM) of standard cylindrical samples (25 mm diameter × 22 mm height) was analyzed using a 2G Enterprises cryogenic rock mag-
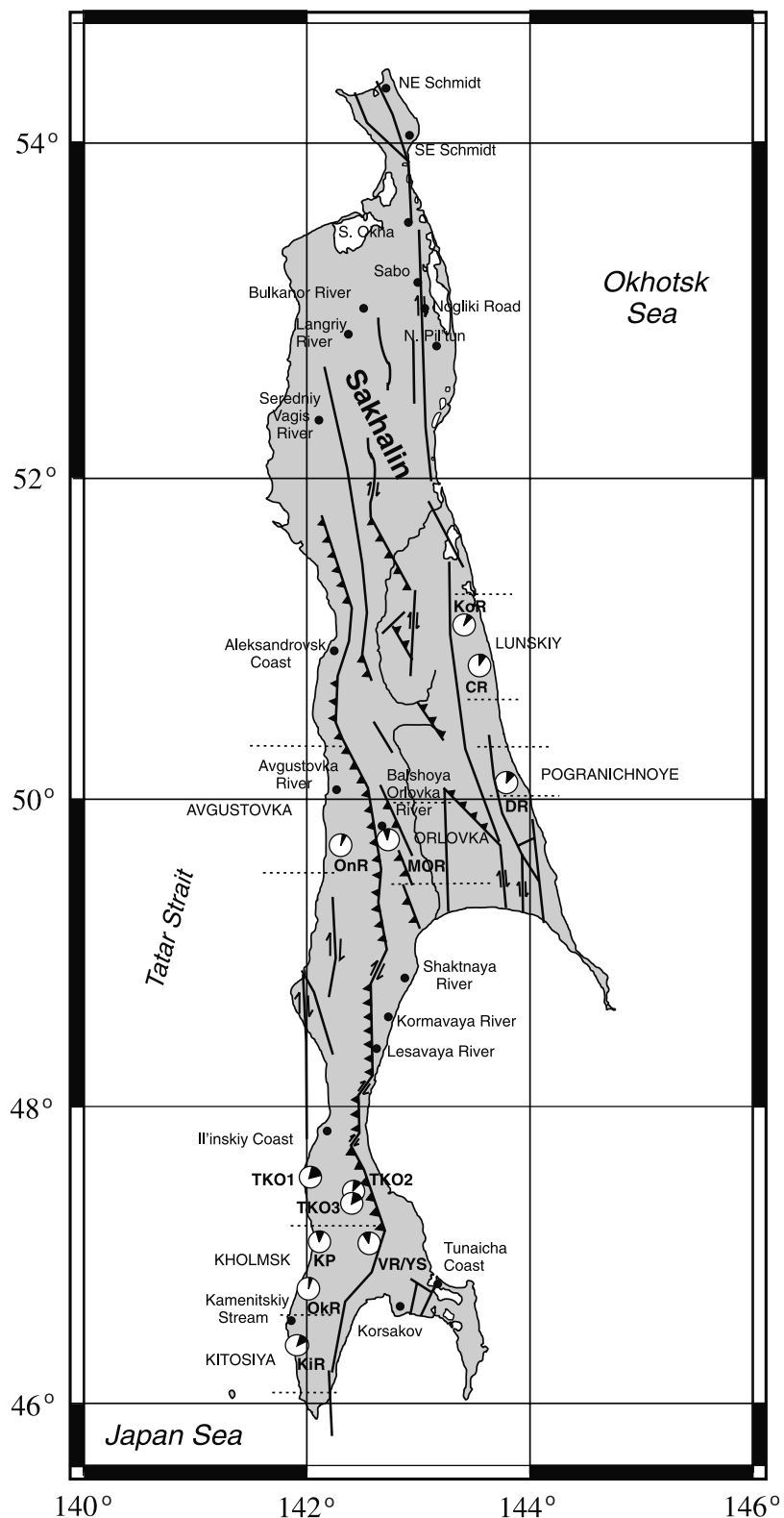
Figure 5. Paleomagnetic sampling localities in Sakhalin. Paleomagnetic declination data from the localities with reliable data are indicated, along with the associated 95% confidence limits. Abbreviations are KiR, Kitosiya River; OkR, Okhta River; KP, Kholmsk Pass; VR/YS, Vladimirovka River and Yar Stream; OnR, Onnay River; MOR, Malaya Orlovka River; DR, Dvoynoye River; CR, Chamgu River; KoR, Kongi River. Localities from *Takeuchi et al.* [1999] are indicated by TKO1, TKO2, and TKO3, respectively. Sites from which no useful paleomagnetic data were obtained are shown as small solid circles.

Table 1. Sampling Localities, Geological Suites, and Description of Local Geology[a]

Locality and Lat./Long.	Number of Samples	Description of Strata and Local Structure			
		Suite	Age	Lithology and Environment	Structure
West Region					
Kitosiya River 46.4°N, 141.9°E	15	Sinegorian Beds	early Paleocene	lagoonal/brackish mudstone and siltstone, intermittent marine sandstone, coal	dip 31°W/187°
Okhta River 46.9°N, 142° E	31	Nevel'sk	early Miocene	marine mudstone and siltstone, volcanic clasts common	dip 50°W/180°
Kholmsk Pass 47.1°N, 142.1°E	49	Takaraday	early Oligocene	marine siltstone and mudstone	core of large anticline, dip 28°W/158° to 2°SE/040°, flanked by the Arakay and Kholmsk suites
		Arakay	Oligocene	mudstone, siltstone, sandstone, volcaniclastics and conglomerate	
		Kholmsk	early Miocene	marine siltstone, sandstone, volcaniclastics and conglomerate	
Vladimirovka R. 47.1°N, 142.3°E	60	Kholmsk	early Miocene	marine mudstone, siltstone, sandstone, volcaniclastics and conglomerate	vertical-overturned strata close to CSF, dip 70°SE/020° to 80°NW/204°
Onnay River 49.6°N, 142.2°E	47	Arakay	Oligocene	marine siliceous mudstone, siltstone, sandstone and conglomerate	east limb of syncline, dip 40°W/193° to 80°W/193°
Central Region					
M. Orlovka River 49.7°N, 142.7°E	27	Nutov	Miocene-Pliocene	marine/deltaic siltstone and sandstone	NW trending syncline, dip 76°NE/330° to 22°SW/114°
East Region					
Dvoynoye River 50.1°N, 143.7°E	25	Lyukamen	Eocene	marine mudstone and sandstone	dip 15°NW/215°
Kongi River 51.1°N, 143.4°E	46	Borsk	early Miocene	marine sandstone and volcaniclastics	dip 65°E/355°
Chamgu River 50.9°N, 143.5°E	25	Borsk	early Miocene	marine siliceous mudstone	dip 48°W/175°

[a]For locations, see Figure 5. CSF, Central Sakhalin Fault. Number of samples refers to the total number of analyzed samples. The number of samples with stable magnetizations are shown in Table 2.

netometer at the Southampton Oceanography Centre (SOC), U.K., and at the Istituto Nazionale di Geofisica e Vulcanologia (INGV), Rome, Italy. All analyzed samples were subjected to progressive demagnetization with a minimum of 10 steps until the samples were almost fully demagnetized and a characteristic remanent magnetization (ChRM) component was isolated or until magnetometer noise levels were reached. The samples measured at SOC were individually measured in four orientations and then remeasured in four orientations in the opposite direction before averaging to ensure directional consistency and precision. It was not possible to follow this procedure at INGV, but the reproducability of results was checked and an accuracy of $1-2°$ was attained for consecutive runs. Pilot samples were measured from every site using thermal and alternating field (AF) demagnetization techniques. Measurement of low-field magnetic susceptibility at each heating step indicated that thermal alteration occurred at elevated temperatures (above 350°C) in almost all samples. Where a ChRM was isolated prior to thermal alteration, the two techniques usually gave comparable results (Figure 6). AF demagnetization was therefore preferred for routine treatment, which was carried out using a tumbling demagnetizing system.

3.2. Paleomagnetic Analyses

[11] Paleomagnetic data were interpreted by least squares principal component analyses of vector component diagrams [*Kirschvink*, 1980]. Statistical treatment of the directional data was carried out using the non-parametric bootstrap method of *Tauxe et al.* [1991]. This statistical framework is ideal for small paleomagnetic data sets ($N < 25$) and makes no assumptions about the initial distribution from which the data were derived. This allows meaningful precision estimates at the 95% confidence level for data sets that are not Fisherian. For Fisherian data sets, the bootstrap calculations approximate the α_{95} estimates calculated following *Fisher* [1953]. For non-Fisherian distributions instead of reporting α_{95} estimates, we report the 95% confidence limits for the semi-axes of the uncertainty ellipse (η_{95}, ζ_{95}) following *Tauxe et al.* [1991].

3.3. Magnetic Properties

[12] A range of rock magnetic measurements was made to identify the magnetic mineral(s) responsible for the paleomagnetic signal at each locality. Anhysteretic remanent magnetizations (ARMs) were imparted to samples from each locality by applying a 0.1 mT DC bias field in the presence of a linearly decaying AF. Partial ARM (pARM) measurements were also made for progressively higher coercivity windows from 5 to 90 mT [e.g., *Jackson et al.*, 1988]. An ARM was first imparted for the range of coercivities up to the upper limit of the required coercivity window; the samples were then AF demagnetized up to the lower limit of the window. The portion of the ARM imparted between the upper and lower limits of the pARM window was then measured using a cryogenic magnetometer at the SOC. Between each pARM measurement, the samples were AF demagnetized at a peak field that was 5 mT higher than the upper limit of the previous step to ensure that the ARM was removed before the next measure-

Table 2. Paleomagnetic Data From Tertiary Rocks, Sakhalin[a]

Locality	Age, Ma	Suite Name	Stratigraphic Thickness, m	Average Bedding Dip, deg/Strike, deg	Lat., deg	Long., deg	Pol.	n	Geographic Coordinates D_m, deg	I_m, deg	α_{95}, deg	k	Fshr?	η_{95}, deg	ζ_{95}, deg	Stratigraphic Coordinates D_m, deg	I_m, deg	α_{95}, deg	k	Fshr?	η_{95}, deg	ζ_{95}, deg
West Sakhalin																						
Kitosiya River	64–60	Sinegorian Beds	~7.2	31 W/187	46	141.9	R + N	14	242.1	−34.0	6.6	37	yes	-	-	218.6	−56.4	6.6	37	yes	-	-
							N	2	-	-	-	-	-	-	-	-	-	-	-	-	-	-
							R	12	241.6	−32.5	7.2	37	yes	-	-	219.7	−54.6	7.2	38	-	-	-
Okhta River	21–17	Lower Nevel'sk	~43	50 W/180	47	142.0	R	9	215.3	−60.0	5.8	81	yes	-	-	179.7	−66.2	3.9	177	yes	-	-
Kholmsk Pass	33–23	Takaraday, Arakay, Kholmsk	~16	28 W/158 to 2 SE/040	47	142.1	N	38	25.5	68.3	6.1	15	no	5.8	5.9	3.4	73.1	5.7	18	no	4.3	5.3
Yar/Vladimirovka River	23–15	Kholmsk	~500	70 SE/020 to 80 NW/204	47	142.3	R + N	13	148.0	17.2	16.7	7	no	5.6	11.9	169.5	−56.7	9.0	22	yes	-	-
Bykov[b]	44–30	L. Due, Krasnopolev, Takaraday	-	-	47	142.5	N	6	321.6	10.7	17.1	16	no	5.1	17.5	353.1	61.0	20.2	12	yes	-	-
							R	7	154.8	39.7	8.7	49	yes	-	-	167.1	−53.1	7.3	69	yes	-	-
							N	63	-	-	-	-	-	-	-	16.7	55.6	8.9	40	yes	-	-
Serpyanka River[b]	28–24	Arakay	-	-	47	142.4	N	53	-	-	-	-	-	-	-	31.8	52.2	13.1	20	yes	-	-
Chekov[b]	24–16	Kholmsk, Nevel'sk	-	-	47	142.2	N	66	-	-	-	-	-	-	-	40.3	58.1	14.4	16	yes	-	-
Onnay River	30–22	Takaraday, Arakay	~209	40 W/193	50	142.2	N	21	59.6	54.3	10.5	10	no	3.4	14.1	14.1	60.7	3.9	67	no	2.6	4.7
Central Sakhalin																						
Malaya Orlovka River	11–2	Nutov	~53	76 NE/330 to 22 SW/114	50	142.7	R	16	112.0	−32.6	15.3	7	no	5.6	19.0	176.5	−48.9	7.7	24	yes	-	-
East Sakhalin																						
Dvoynoye River	47–41	Lyukamen	~304	15 NW/215	50	143.7	R	12	220.0	−57.5	14.6	12	no	7.9	10.0	211.8	−54.2	11.1	16	yes	-	-
Changu River	24–20	Lower Borsk	~9.1	48 W/175	51	143.5	R	17	238.6	−28.9	7.4	24	yes	-	-	200.6	−66.0	7.4	24	yes	-	-
Kongi River	11–5	Upper Borsk	~17	65 E/355	51	143.4	R	20	121.7	−37.7	6.4	20	no	4.5	7.4	205.0	−55.7	6.4	27	no	4.5	7.4

[a]Pol., polarity, N, normal, or R, reversed; Fshr?, are the data Fisher distributed?
[b]Data from *Takeuchi et al.* [1999].

ment. Low-temperature magnetic properties were analyzed using a Quantum Design Magnetic Properties Measurement System (MPMS-XL5) at the Institute for Rock Magnetism, Minnesota. Zero-field-cooling (ZFC) experiments were carried out by cooling a sample to 20 K in zero field, applying a field of 2.5 T and then switching off the field before measuring the low-temperature IRM during heating back to 300 K. These measurements helped with identification of the magnetic mineral(s) responsible for the NRM and help to assess the reliability of the ChRM in the samples. Thermomagnetic curves were obtained for bulk sediment samples using a variable field translation balance with a field of 76 mT and a heating rate in air of 10°C/min up to 700°C. Thermal alteration affected most samples and no mineralogically diagnostic data were obtained.

[13] In addition, an impulse magnetizer was used to impart an isothermal remanent magnetization (IRM) to a selection of three to seven samples from each locality at increasing fields up to 0.8 T to assess the significance of magnetic remanence anisotropy. The field was applied at 45° to the bedding plane, to avoid any field impressed anisotropy [*Tauxe et al.*, 1990], and the IRM was then measured parallel (IRM$_x$) and perpendicular (IRM$_z$) to bedding.

[14] The anisotropy of magnetic susceptibility (AMS) was measured using an AGICO Kappabridge KLY 3S magnetic susceptibility meter on samples from localities with well-defined paleomagnetic data. Measurements were made in rotational mode to evaluate the susceptibility in 3 orthogonal planes, at the INGV, Rome, Italy. The measurements allow evaluation of the percentage anisotropy, the shape of the anisotropy ellipsoid, and the dominant magnetic fabric. This can be important in sedimentary rocks where compaction can affect the orientation of magnetic grains at around the time of magnetization lock-in [*Blow and Hamilton*, 1978].

4. Results

4.1. West Sakhalin

4.1.1. Kitosiya River

[15] Eight samples from Kitosiya River were subjected to thermal demagnetization. AF demagnetization was performed on the remaining samples. Thermal and AF demagnetization reveal the same component of magnetization (Figures 6a and 6b). A stable reversed polarity ChRM was found in 12 samples, and a normal polarity ChRM was identified in two samples (Figure 7a). A weak normal polarity viscous overprint is evident in some samples, probably due to exposure in the present-day geomagnetic field (Figure 6a). Rapid decay of the magnetization to near-zero levels at around 360°C suggests that a magnetic iron sulfide may be present in some of the samples. The Verwey-transition, which is identified by an anomaly at around 120 K in low-temperature data, indicates that magnetite is present (Figure 8). High relative pARM intensities below 20 mT, and a second peak at 30 mT, confirms that a range of magnetite grain sizes is likely to be present from pseudo-single-domain (PSD) sizes of 2–3 μm, to multidomain (MD) sizes of around 5–25 μm [*Jackson et al.*, 1988] (Figure 9). The paleomagnetic directions for the magnetite and inferred sulfide NRM components are indistinguishable, therefore, it is likely that both components locked in at

a similar time. The data are insufficient for a reversals test (Figure 7a), but the presence of normal and reversed polarity data suggests that the sampled interval is thick enough to have enabled averaging of geomagnetic secular variation. The ChRM is interpreted as a primary magnetization, with a locality-mean direction of $D_m = 218.6°$, $I_m = -56.4°$, with $\alpha_{95} = 6.6°$ (Figure 7a and Table 2).

4.1.2. Okhta River

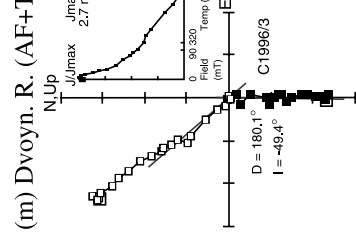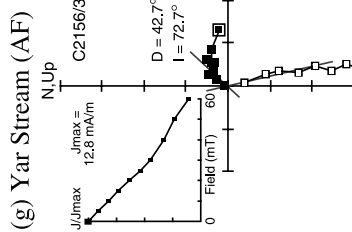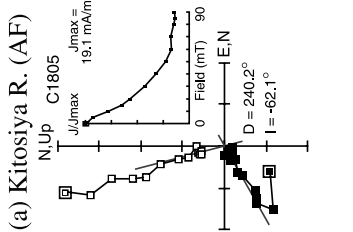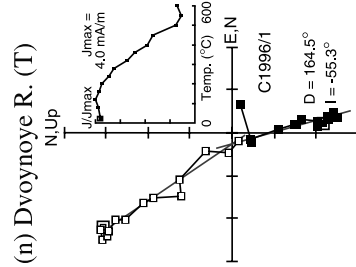[16] Samples from Okhta River have both stable normal and reversed polarity ChRM directions, which are usually isolated after removal of a secondary normal polarity component (Figure 6c). *Weaver et al.* [2002] demonstrated that the normal polarity samples carry a synfolding magnetization, while the reversed polarity samples are consistent with a geocentric axial dipole direction at the site latitude. On the basis of detailed rock magnetic and electron microscopic investigations of polished sections, they showed that the synfolding magnetization in the normal polarity samples is carried by pyrrhotite, which the evidence suggests formed in association with a late diagenetic fluid migration event. For the reversed polarity samples, thermal demagnetization appears to reveal the same compon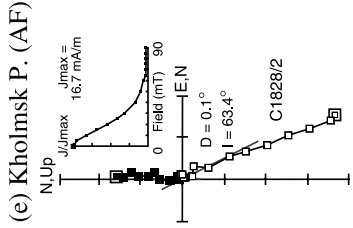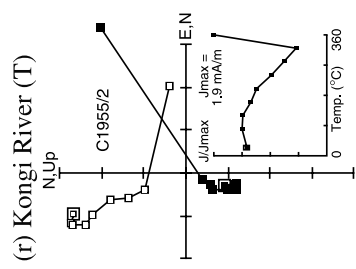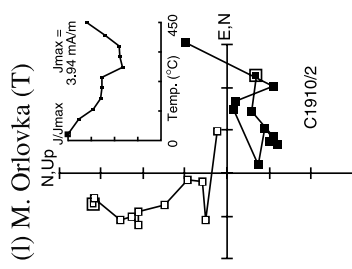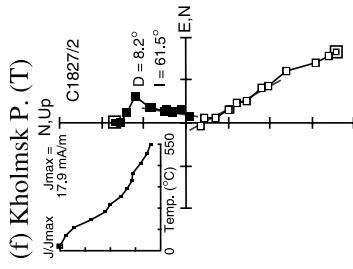ent of magnetization identified with AF demagnetization, although the thermal data are noisier (Figure 6d). Low-titanium magnetite appears to be the primary remanence carrier because the NRM falls to near-zero values at around 550°C (Figure 6d). Low-temperature data contain evidence of a weak Verwey transition, which suggests that magnetite is present (Figure 8). Partial ARM data suggest that PSD magnetite grains probably carry the remanence in the reversed polarity samples from Okhta River (Figure 9). The reversed polarity ChRM and improved clustering after tilt correction (Table 2) suggests that these directions are primary. Locality-mean values are $D_m = 179.7°$, $I_m = -66.2°$, with $_9\alpha_5 = 3.9°$ (Figure 7b and Table 2).

4.1.3. Kholmsk Pass

[17] Useful paleomagnetic data were obtained for 38 samples from Kholmsk Pass. Stable magnetizations are discernable after removal of viscous magnetic overprints which are present in many samples (Figures 6e and 6f). Thermal demagnetization of pilot samples suggests that a low-titanium magnetite is probably the magnetic carrier, because most of the NRM is removed below 550°C (Figure 6f). Data from pARM experiments show a peak at 30 mT, which is consistent with the presence of PSD magnetite (Figure 9). Furthermore, identification of the Verwey transition at around 120 K indicates that magnetite is present (Figure 8). The locality-mean ChRM is $D_m = 3.4°$, $I_m = 73.1°$, with $\eta_{95} = 4.3°$ and $\zeta_{95} = 5.3°$ (Figure 7c). A bootstrap fold test [*Tauxe and Watson*, 1994] was carried out on the data from Kholmsk Pass (Figure 10a). This analysis reveals that maximum clustering occurs at around 80% unfolding, however, the 95% confidence limit on this direction ranges from 49% to 98% unfolding. The test is, therefore, inconclusive because the 95% confidence region eliminates the possibility of accurately constraining the timing of remanence acquisition. Slightly improved clustering after full tilt correction suggests that the ChRM is likely to be primary (Table 2).

4.1.4. Yar Stream/Vladimirovka River

[18] Samples from Yar Stream and Vladimirovka River, located about 1 km east of the central fault region in south

Figure showing orthogonal vector (Zijderveld) demagnetization diagrams and normalized intensity decay plots for samples from various Sakhalin localities:
(a) Kitosiya R. (AF) — C1805, D = 240.2°, I = -62.1°, Jmax = 19.1 mA/m
(b) Kitosiya R. (T) — C1803, D = 247.3°, I = -44.9°, Jmax = 1.6 mA/m
(c) Okhta River (AF) — C2500/4, D = 192.0°, I = -72.3°, Jmax = 5.5 mA/m
(d) Okhta River (T) — C2502/1, Jmax = 1.1 mA/m
(e) Kholmsk P. (AF) — C1828/2, D = 0.1°, I = 63.4°, Jmax = 16.7 mA/m
(f) Kholmsk P. (T) — C1827/2, D = 8.2°, I = 61.5°, Jmax = 17.9 mA/m
(g) Yar Stream (AF) — C2156/3, D = 42.7°, I = 72.7°, Jmax = 12.8 mA/m
(h) Yar Stream (T) — C2167/3, Jmax = 0.5 mA/m
(i) Onnay River (AF) — C1887/4, D = 0.3°, I = 66.8°, Jmax = 5.21 mA/m
(j) Onnay River (T) — C1885/2, Jmax = 4.74 mA/m
(k) M. Orlovka (AF) — C1910/5, D = 191.6°, I = -53.5°, Jmax = 5.31 mA/m
(l) M. Orlovka (T) — C1910/2, Jmax = 3.94 mA/m
(m) Dvoyn. R. (AF+T) — C1996/3, D = 180.1°, I = -49.4°, Jmax = 2.7 mA/m
(n) Dvoynoye R. (T) — C1996/1, D = 164.5°, I = -55.3°, Jmax = 4.0 mA/m
(o) Chamgu R. (AF) — C1986/1, D = 247.4°, I = -44.5°, Jmax = 3.7 mA/m
(p) Chamgu R. (T) — C1986/1, Jmax = 18.6 mA/m
(q) Kongi River (AF) — C1950/1, D = 185.8°, I = -53.9°, Jmax = 2.0 mA/m
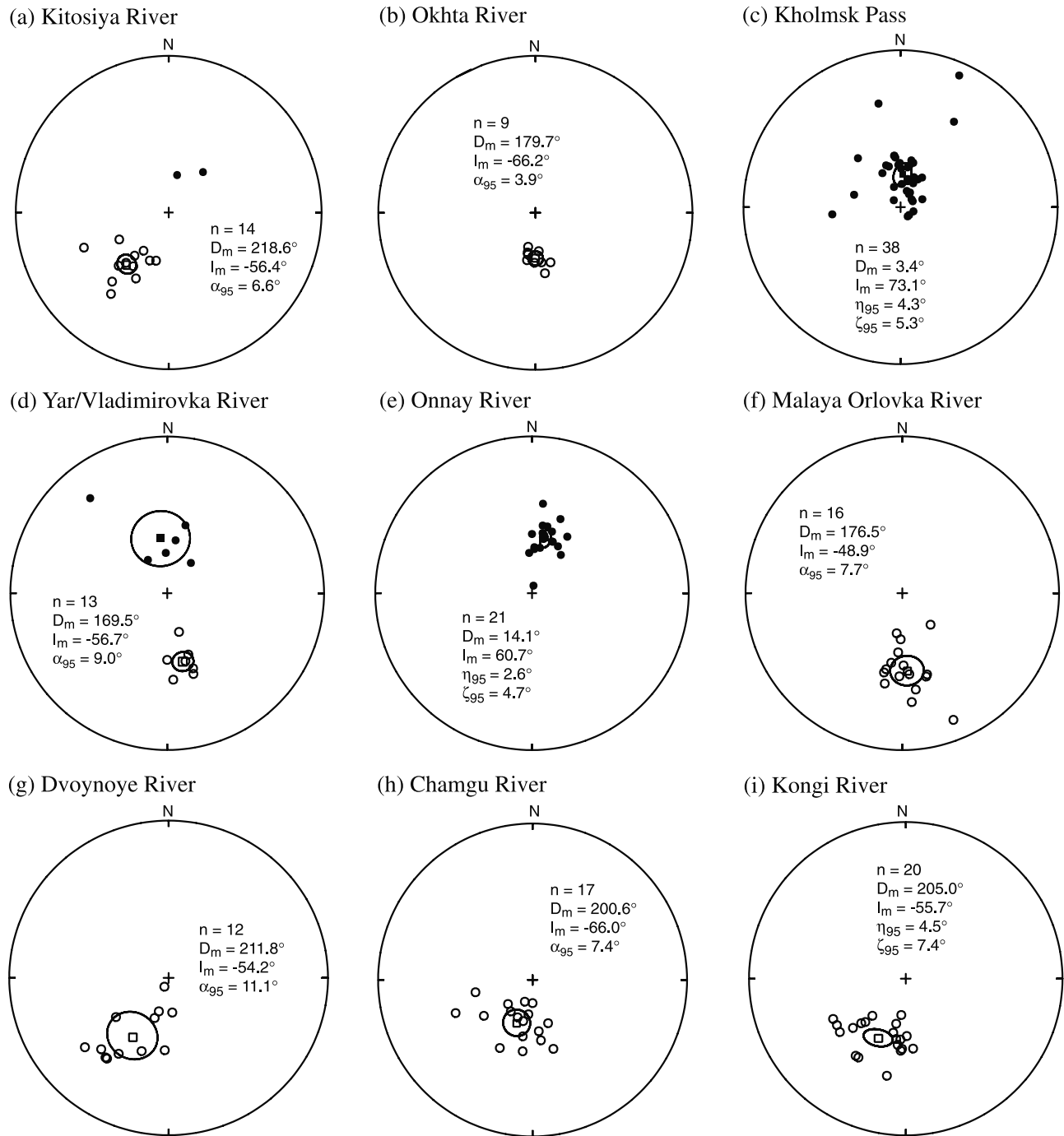(r) Kongi River (T) — C1955/2, Jmax = 1.9 mA/m

Figure 7. Equal-area stereographic plots showing the site-mean remanence directions from Sakhalin. Reversed and normal polarity sites are plotted. Square represents the mean paleomagnetic direction (n is number of samples with stable magnetizations; D_m is mean declination; I_m is mean inclination). The ellipses represent the 95% confidence limit defined by the α_{95} value [see *Fisher*, 1953] or by η_{95} and ζ_{95} for the 95% confidence limits that define the minor and major semi-axes for confidence ellipses determined using bootstrap statistics for non-Fisherian data sets [*Tauxe et al.*, 1991].

Figure 6. (opposite) Vector component plots for representative samples from Sakhalin, with plots of magnetization decay on demagnetization. Lines represent least squares best fits to the ChRM vector [*Kirschvink*, 1980]. Open symbols represent projections onto the vertical plane (inclinations), and solid symbols represent projections onto the horizontal plane (declinations). All data are shown after structural tilt correction.
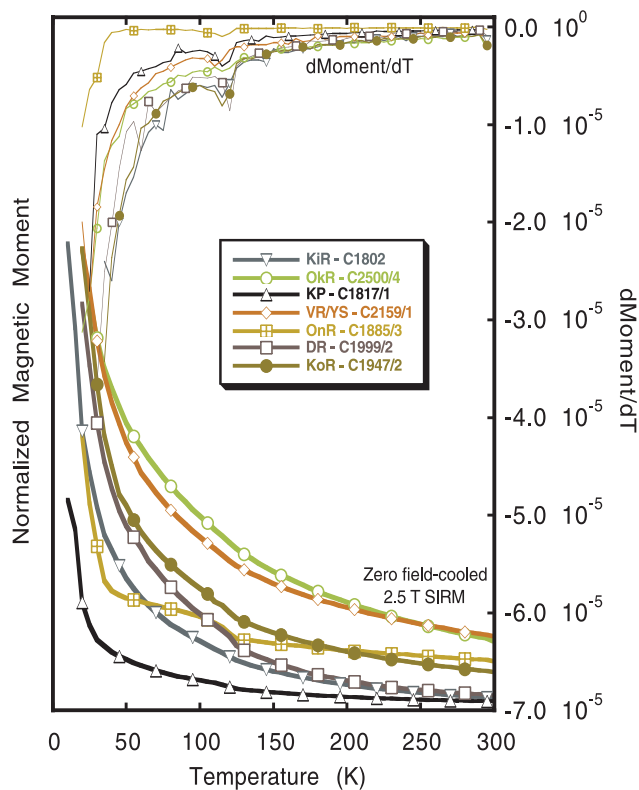
Figure 8. Low-temperature ZFC plots (normalized magnetic moment versus temperature), with the first derivative of the curves shown above. The Verwey transition, which is characteristic of magnetite, is detected at around 120 K for all samples.

Sakhalin (Figure 5), were sampled in exposures of the early Miocene Kholmsk Suite. A stable ChRM component was revealed for some samples by AF demagnetization above 25 mT (Figure 6g). Thermal demagnetization was carried out on pilot samples, but mineral alteration was evident at around $300-400°C$ (Figure 6h). Both normal and reversed polarity ChRM directions were observed in 13 mudstone samples, some of which were from overturned beds (Figure 7d). Low-temperature SIRM data and pARM acquisition data suggest that PSD magnetite is the dominant remanence carrier at this locality (Figures 8 and 9). The tilt-corrected ChRM has a locality-mean direction of $D_m = 169.5°$, $I_m = -56.7°$, with $\alpha_{95} = 9.0°$ (Figure 7d and Table 2). A bootstrap fold test was carried out on the data, which indicates a best-clustering direction that includes the 100% unfolded direction (Figure 10b). The reversed and normal polarity data also pass a bootstrap reversals test [*Tauxe et al.*, 1991]. The ChRM is therefore interpreted to be primary.

4.1.5. Onnay River

[19] A stable normal polarity ChRM was identified in 21 samples from Onnay River (Figure 7e). Thermal and AF demagnetization data are comparable before thermal alteration occurs at 220°C (Figures 6i and 6j). A small amount of the NRM remains after AF demagnetization at 140 mT, which suggests that a high-coercivity magnetic mineral is present. However, a Verwey transition indicates that magnet-

ite is present (Figure 8). A pARM peak at 30 mT suggests that the magnetite occurs as PSD ($\sim 2-3$ μm) grains (Figure 9). Random paleomagnetic directions from 11 samples obtained from an intraformational conglomerate at the top of the sampled sequence suggest that the magnetic remanence is ancient (i.e., it predates the conglomerate). The resultant vector length R for the conglomerate data is 3.02, which is less than the critical value of $R_{95} = 5.29$ for n = 11 [*Watson*, 1956], above which non-randomness cannot be disproved at the 95% confidence level (Figure 10c). The locality-mean direction is $D_m = 14.1°$, $I_m = 60.7°$, with $\eta_{95} = 2.6°$ and $\zeta_{95} = 4.7°$ (Figure 7e).

4.2. Central Sakhalin

[20] Sixteen samples from Malaya Orlovka River yielded stable paleomagnetic directions. A reversed polarity ChRM is identified between 30 and 65 mT, after removal of a normal polarity overprint (Figure 6k). Thermal demagnetization experiments indicate thermal alteration of the magnetic minerals at around 350°C. Thermal and AF demagnetization results are similar before the onset of thermal alteration
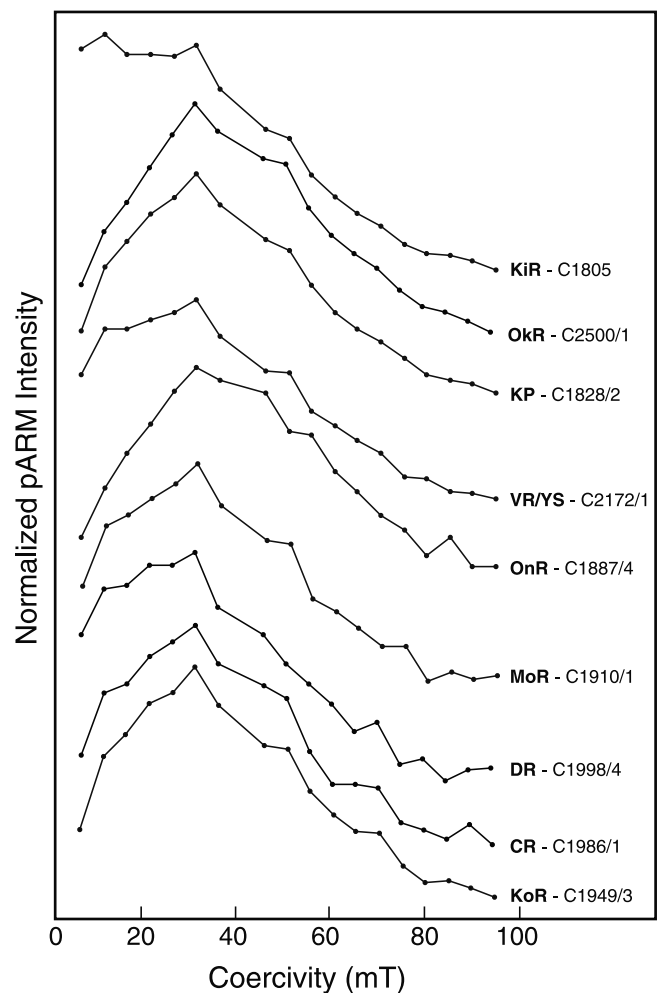

Figure 9. Partial ARM spectra for representative samples from all sampling localities (same abbreviations as in Figure 5). Peak values at around 30 mT suggest that PSD magnetite is the greatest contributor to the remanence [*Jackson et al.*, 1988].
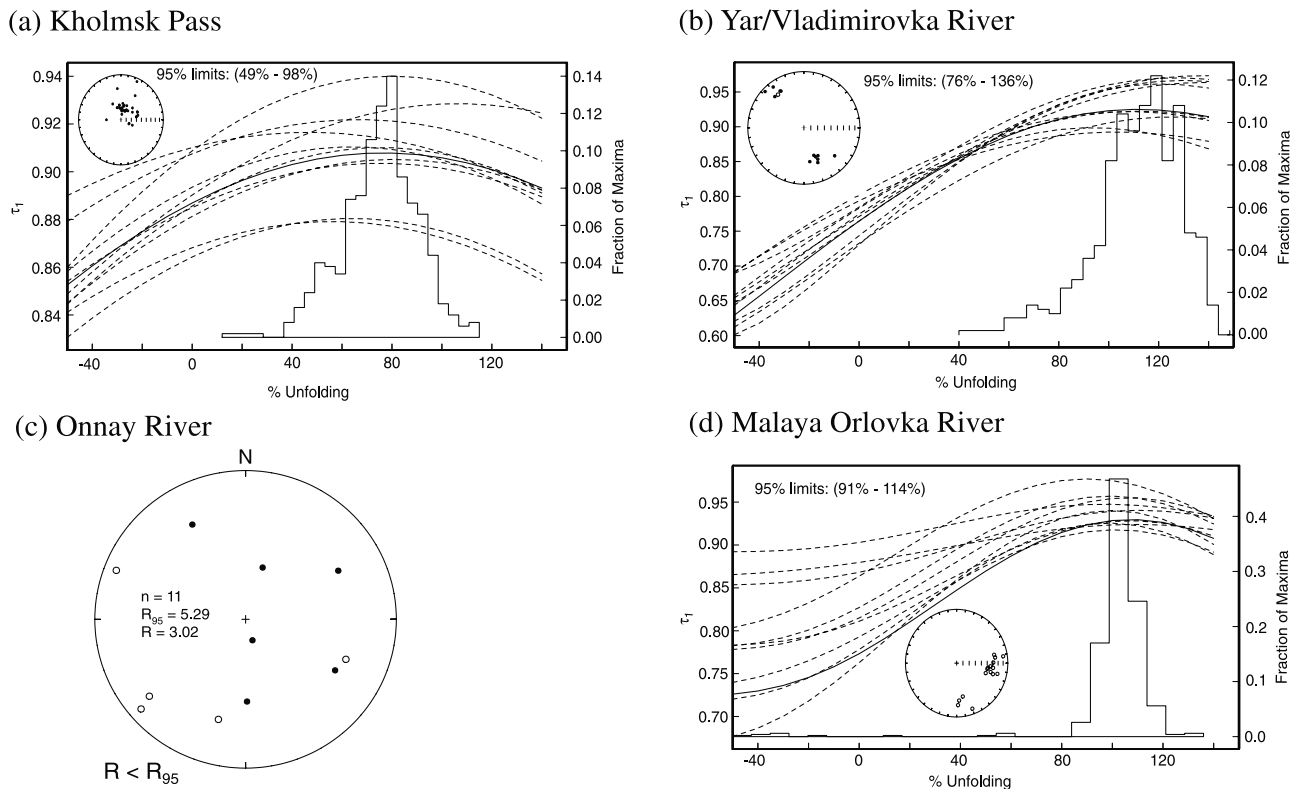
(a) Kholmsk Pass   (b) Yar/Vladimirovka River

(c) Onnay River   (d) Malaya Orlovka River

Figure 10. Paleomagnetic field tests. (a) and (b) Bootstrap fold tests following the method of *Tauxe and Watson* [1994] for data from Kholmsk Pass and Yar Stream/Vladimirovka River, respectively. Principal eigenvalues of paleomagnetic data are plotted for varying percentages of structural unfolding. (c) Conglomerate test for intraformational conglomerate at Onnay River (plotted in geographic coordinates). Randomness cannot be disproved at the 95% confidence level [*Watson*, 1956], and the test is passed. (d) Bootstrap fold test for data from Malaya Orlovka River.

(Figures 6k and 6l). A clear peak is present at 30 mT in pARM acquisition plots, with rapid decay of the remanence in higher-coercivity windows (Figure 9). It is therefore likely that the remanence is dominated by PSD magnetite [*Jackson et al.*, 1988]. The data pass a bootstrap fold test (Figure 10d). A well-defined peak at 100% unfolding suggests that the ChRM is primary. The mean paleomagnetic direction for the locality is $D_m = 176.5°$, $I_m = -48.9°$, with $\alpha_{95} = 7.7°$ (Figure 7f).

4.3. Northeast Sakhalin

4.3.1. Dvoynoye River

[21] At Dvoynoye River, paleomagnetic data from 12 samples have a stable high-coercivity ChRM. AF demagnetization had little effect in removing the NRM above 90 mT, so thermal demagnetization was carried out to remove the remaining NRM up to 700°C (Figure 6m). In other cases, the NRM was virtually removed at around 550°C (Figure 6n). The paleomagnetic direction isolated by AF demagnetization is identical to that isolated using thermal demagnetization (Figures 6m and 6n). A minor low-coercivity viscous component is observed in some samples possibly due to laboratory storage (Figures 6m and 6n). A Verwey transition indicates that magnetite is present in the samples (Figure 8) and a peak in the pARM data at 30 mT suggests that the magnetite is in the PSD size range (Figure 9). Thus it appears that magnetite is the dominant rema-

nence carrier, together with a high-coercivity mineral. The high-coercivity mineral is probably hematite since part of the remanence persists to 650–700°C. The hematite appears to be present in variable concentrations in different samples. All samples have reversed polarity and give a locality-mean direction of $D_m = 211.8°$, $I_m = -54.2°$, with $\alpha_{95} = 11.1°$ (Figure 7g and Table 2).

4.3.2. Chamgu River

[22] For Chamgu River, 17 paleomagnetic samples yielded a stable ChRM above 25 mT (Figure 6o). A low-coercivity overprint with variable directions is also present. The overprint is probably a viscous magnetization acquired in the present-day geomagnetic field or in the laboratory. Thermal demagnetization below 300°C reveals the same component of magnetization as AF demagnetization; thermal alteration occurs above this temperature (Figure 6p). Partial ARM data indicate a clear peak at 30 mT, which suggests that PSD magnetite is responsible for the NRM (Figure 9). A reversed polarity ChRM suggests that recent remagnetization has not occurred and the ChRM direction is interpreted as a primary magnetic component. The locality-mean paleomagnetic direction for the ChRM components calculated from these samples is $D_m = 200.6°$, $I_m = -66.0°$, with $\alpha_{95} = 7.4°$ (Figure 7h and Table 2).

4.3.3. Kongi River

[23] Twenty samples from Kongi River yielded stable paleomagnetic directions. Most of the samples were from

tuffaceous beds. A high-coercivity (25–120 mT) ChRM component has reversed polarity and is interpreted as a primary magnetization (Figure 6q). Viscous overprints are present in many samples below 25 mT. A Verwey transition at 120 K indicates the presence of magnetite (Figure 8). Similar results were obtained using AF and thermal demagnetization, although thermal alteration prevented heating above 360°C in tuffaceous samples (Figures 6q and 6r). Rapid thermal decay of the remanence below 360°C in tuffaceous samples (Figure 6r) is probably due to a titanomagnetite, although the AF demagnetization results also suggest the presence of a high-coercivity iron-oxide mineral such as hematite (Figure 6q). Partial ARM acquisition results indicate a peak at 30 mT, which, together with the thermal demagnetization data, suggests that PSD titanomagnetite is likely to be the primary NRM carrier (Figure 9). The mean paleomagnetic direction for the Kongi River locality is $D_m = 205.0°$, $I_m = -55.7°$, with $\eta_{95} = 4.5°$ and $\zeta_{95} = 7.4°$ (Figure 7i and Table 2).

5. Discussion

[24] Several kinematic models have been proposed for the evolution of NE Asia [e.g., *Otofuji et al.*, 1991; *Jolivet et al.*, 1994; *Altis*, 1999]. The models covering the Okhotsk Sea region are primarily derived using data from Japan and the Japan Sea. However, because geological data are sparse for both Sakhalin and the Okhotsk Sea, the models are poorly constrained and inconsistent and the geodynamic evolution of this region remains unclear. Analysis of paleomagnetic data can help to constrain tectonic models in several ways. First, the data can constrain the timing of deformation. Second, they can help evaluate whether Sakhalin has evolved with the Pacific, North American or Eurasian plates and they can help identify the position of plate boundaries which are currently unclear (e.g., Figure 2). Third, the data can be used to delineate local domains with similar deformation history. Fourth, they can help define the structural style of deformation and hence provide insights into the tectonic evolution of the region. In the following, we discuss the geodynamic implications of paleomagnetic data from Sakhalin and the constraints they place on kinematic models of the regional dynamics.

5.1. Tertiary Paleolatitudinal Evolution of Sakhalin
5.1.1. Paleomagnetic Inclination Data

[25] A Mesozoic accretionary complex in east Sakhalin indicates that the early geological evolution of Sakhalin was linked with the Pacific Plate, at least until the Eocene after final emplacement of an allochthonous terrane in southeast Sakhalin [*Bazhenov et al.*, 2001]. Currently, the Okhotsk Sea separates Sakhalin from the subducting Pacific Plate (Figure 1). Thus there has been a transition within the Cenozoic between a geological evolution associated with the Pacific Plate and evolution with some other plate(s). Comparison of paleomagnetic inclination data for Tertiary rocks from Sakhalin with the APWPs for the Pacific, Eurasian, and North American plates (Figure 11) can help to constrain the timing of this transition. Inclination data from Oligocene beds at Kholmsk Pass are significantly different from the Pacific Plate APWP and are in good agreement with the North American and Eurasian APWPs
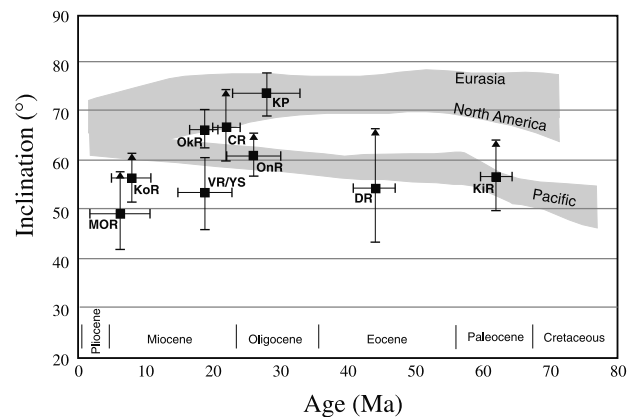

Figure 11. Inclination versus age for paleomagnetic data from Sakhalin compared with the Eurasian, North American [*Besse and Courtillot*, 1991], and Pacific [*Gordon and Van der Voo*, 1995] reference plates. The reference directions expected for a geocentric axial dipole (GAD) field are plotted as a shaded envelope for the latitudinal range of Sakhalin. Arrows indicate probable inclination shallowing; the inclinations should be steeper to be representative of the paleofield (see Figures 12 and 13). Localities are indicated using the same abbreviations as in Figure 5.

(Figure 11). This might suggest that the transition occurred by Oligocene time. However, data from Chamgu River and Okhta River have 95% confidence error bars that span the North American, Eurasian and Pacific Plate APWPs. The data for the Kongi River, Vladimirovka/Yar Stream and Dvoynoye River localities plot within error of the Pacific Plate APWP, while mean inclination data from Onnay River and Kitosiya River plot directly in agreement with the Pacific path. Inclinations from Malaya Orlovka do not plot within error of any of the APWPs used for comparison in Figure 11, and are anomalously shallow. A number of depositional mechanisms can cause the long axes of naturally anisotropic magnetic remanence bearing particles to rotate toward the bedding plane in a sediment [*Arason and Levi*, 1990]. Placing further constraint on the Tertiary evolution of Sakhalin appears to be difficult without testing for possible inclination shallowing within the studied sedimentary rocks.

5.1.2. Testing for Postdepositional Inclination Shallowing

[26] Initial investigation of inclination shallowing was carried out by measuring the anisotropy of magnetic susceptibility (AMS). In samples where the magnetic fabric is oblate, and the minimum susceptibility (k_{min}) is perpendicular to the bedding plane, an inclination correction can be applied if the susceptibility is dominated by ferrimagnetic minerals [*Hodych et al.*, 1999]. Alternatively, the anisotropy of ARM (AARM) can be measured to make such corrections [*Jackson et al.*, 1991; *Kodama*, 1997; *Tan and Kodama*, 1998]. In both cases, successful correction requires the average anisotropy of magnetic particles to be constant and small [*Hodych and Bijaksana*, 1993].

[27] Samples from Dvoynoye River, Kongi River, and Malaya Orlovka River have oblate AMS ellipsoids and tilt-
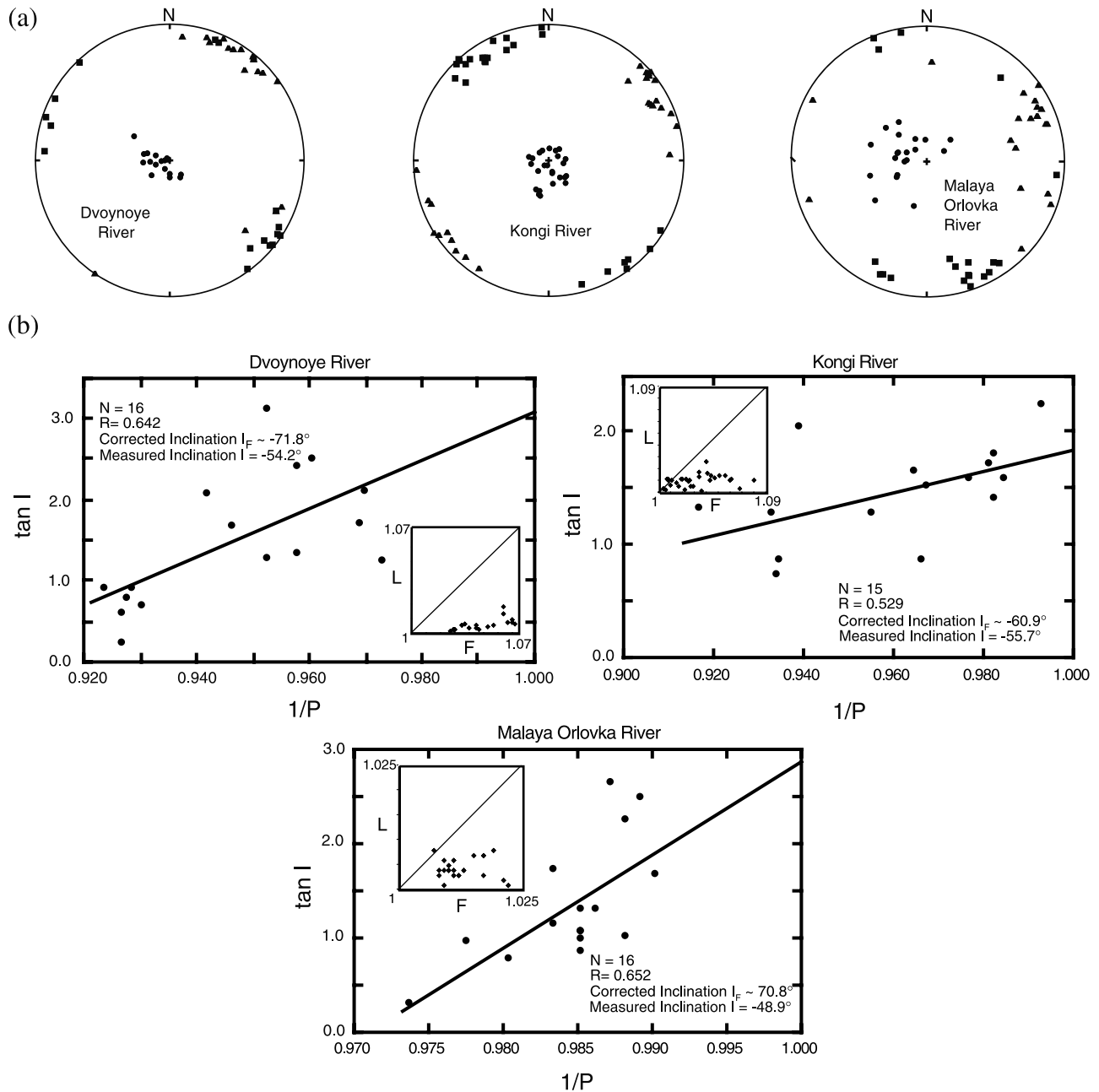
Figure 12. (a) Equal-area plots of magnetic fabrics in stratigraphic coordinates for Dvoynoye River, Kongi River, and Malaya Orlovka River. Dots represent k_{min}, triangles represent k_{int}, and squares represent k_{max}. (b) Prediction of the expected inclination for paleomagnetic samples for the three localities shown in Figure 12a, based on AMS parameters ($P = k_{max}/k_{min}$), following *Hodych et al.* [1999]. Oblate magnetic fabrics are indicated in the Flinn susceptibility plots (L versus F, where $L = k_{max}/k_{int}$ and $F = k_{int}/k_{min}$).

corrected magnetic fabrics with k_{min} axes close to vertical (Figure 12a). Samples from other localities have variable AMS ellipsoid shapes and are therefore unsuitable for direct AMS or AARM correction. There appears to be a significant correlation between tan I and the percentage anisotropy for the three localities (Figure 12b). An AMS-based correction was made following the method of *Hodych et al.* [1999] where the inclination prior to flattening (I_F) is estimated by extrapolating the best fit line to the point where $k_{min}/k_{max} = 1$. Comparison of inclination and I_F

values for these localities suggests an inclination flattening of up to ~20° (Figure 12b). With this method, it is assumed that the magnetic fabric is controlled by ferrimagnetic particles rather than by paramagnetic or diamagnetic matrix minerals. This assumption is not always valid and it is preferable to provide a more direct explanation for inclination shallowing by determining whether the remanence carrying grains are also anisotropic.

[28] An alternative anisotropy test was performed by measuring an IRM parallel (IRM_x) and perpendicular
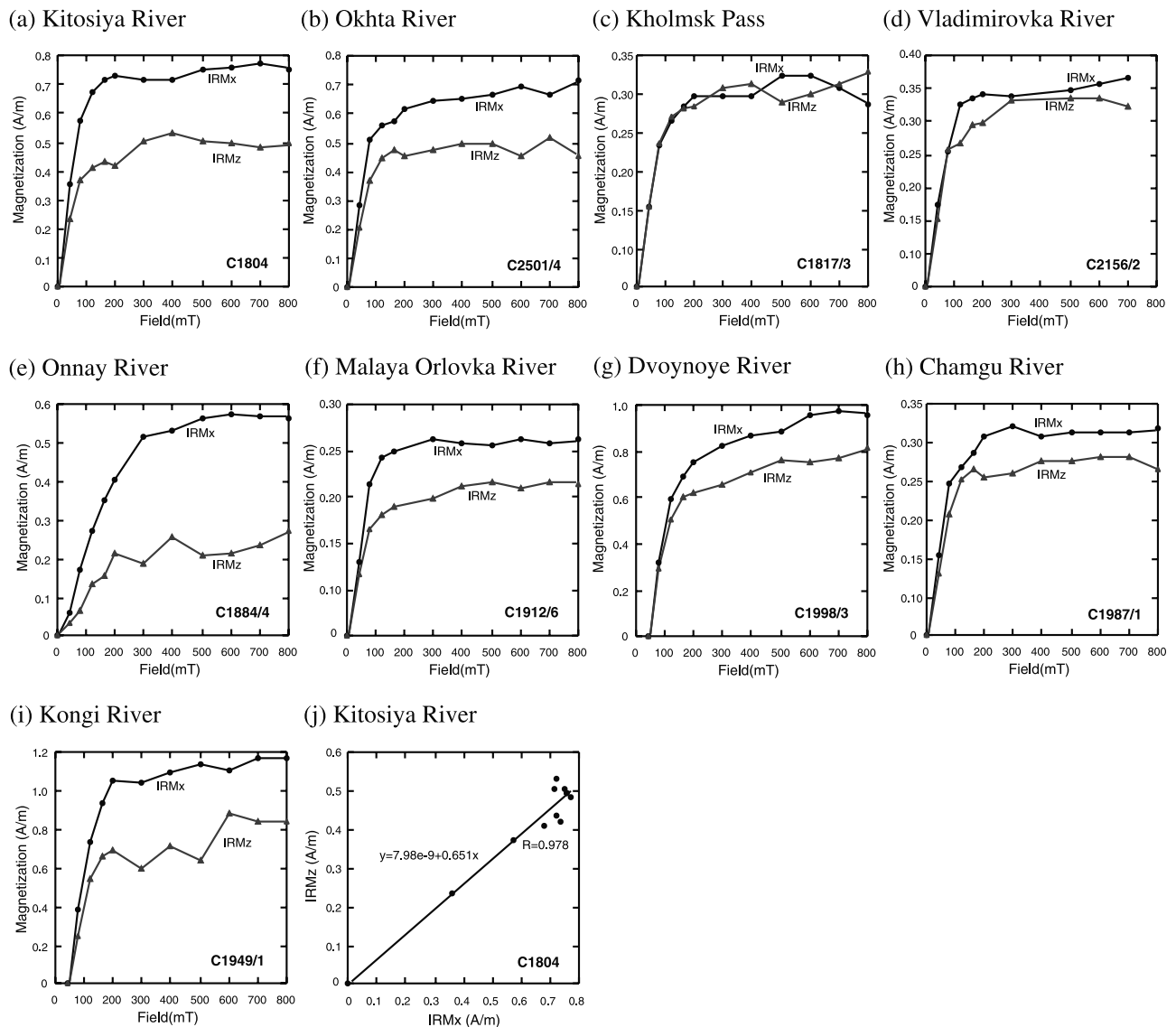
Figure 13. (a)–(i) IRM acquisition curves for bedding-normal components (IRM$_z$) and bedding-parallel components (IRM$_x$) for all successful paleomagnetic sampling localities in Sakhalin. (j) Gradient of the best fit correlation line of IRM$_z$ versus IRM$_x$ used to determine the IRM$_z$/IRM$_x$ ratio, which gives an estimate of inclination shallowing in the sediments [*Hodych and Buchan*, 1994].

(IRM$_z$) to the bedding plane to qualitatively evaluate the possibility of inclination shallowing. Inclination shallowing is manifest when IRM$_z$ is less than IRM$_x$. The ratio IRM$_z$/IRM$_x$ can be related to the amount of inclination shallowing by: tan I/tan I_F = IRM$_z$/IRM$_x$ [*Hodych and Buchan*, 1994]. For the majority of samples analyzed from Sakhalin, the value of IRM$_z$ is lower than IRM$_x$ for the entire range of applied fields (Figure 13). This suggests that the NRM carrying fraction of grains is significantly anisotropic. The average IRM$_z$/IRM$_x$ ratio for each sample was determined from the best fit slope of IRM$_z$ against IRM$_x$ (Figure 13j). Only samples with a correlation coefficient of R > 0.7 were considered in our summary of IRM anisotropy data in Table 3. It is noteworthy that samples from Kholmsk Pass, where there is no discrepancy between the mean inclination value and the Eurasian and North American APWPs (Figure 11), have a mean IRM$_z$/IRM$_x$ ratio close to unity (Table 3 and

Figure 13c). Smaller ratios are found for all other localities, which indicates that inclination shallowing is likely to be significant (Table 3). More rigorous quantification of post-depositional inclination shallowing usually requires determination of the AARM tensor, sediment redeposition and electron microscopic analysis of grain size and shape to assess remanence anisotropy [*Jackson et al.*, 1991; *Kodama*, 1997; *Tan and Kodama*, 1998]. Such detailed analysis is beyond the scope of the present study. We simply indicate the likelihood of inclination shallowing with arrows on the data points in Figure 11, which suggest that these localities should have steeper mean inclinations.

5.1.3.   Paleolatitude Implications of Tertiary Paleomagnetic Data From Sakhalin

[29]   The likelihood of significant inclination shallowing for many of the localities sampled in Sakhalin indicates that post-Paleocene evolution of Sakhalin with the Pacific Plate

Table 3. Anisotropy of IRM Data[a]

Locality	n	IRM_z/IRM_x	Average Flattening, deg
Kitosiya River	6	0.900	6.5
Okhta River	3	0.820	4.1
Kholmsk Pass	6	0.957	1.0
Yar/Vlad. River	5	0.739	4.1
Onnay River	3	0.738	6.0
M. Orlovka River	6	0.669	9.8
Dvoynoye River	7	0.768	7.1
Chamgu River	6	0.447	12.4
Kongi River	5	0.735	8.1

[a]The inclination flattening, $I_F - I$, was determined for each sample and divided by the number of samples (n) to calculate the average flattening.

is improbable. The data are insufficient to enable us to distinguish whether Sakhalin evolved with the Eurasian or the North American plates. However, they do suggest that the sampled localities have remained near present-day latitudes since the mid-Paleocene (Figure 11). If this was the case, the attribution of late Cenozoic volcanism in the area to subduction-related processes [*Zonenshain et al.*, 1990] is incorrect.

## 5.2. Timing of Cessation of Subduction Beneath Sakhalin

[30] Vertical axis rotations, which are detectable by comparing measured paleomagnetic declinations with the expected APWP, are commonly associated with strike-slip fault systems [e.g., *Jackson and Molnar*, 1990; *Little and Roberts*, 1997]. The mean declinations from the localities sampled in Sakhalin are shown in Figures 5 and 14a. The data can be divided into two groups based on their common deformational history: (1) east Sakhalin (Figure 14b) and (2) localities in Sakhalin to the west of, and in the vicinity of, the Central Sakhalin Fault (Figure 14c). The expected declinations for the North American and Eurasian Plates are also shown.

[31] In east Sakhalin, there appears to have been approximately 10° of relative clockwise rotation from the middle Eocene to the early Miocene (Figure 14b). This is the earliest indication of a possible right-lateral strike-slip tectonic regime [*Fournier et al.*, 1994]. It suggests that Pacific Plate subduction had probably ceased by the onset of this rotation, which is consistent with Eocene accretion of a Pacific Plate allochtonous terrane in southeast Sakhalin [*Bazhenov et al.*, 2001]. This terrane accreted against Sakhalin on the Tonino-Aniva Peninsula (Figure 1b),

Figure 14. (opposite) Declination versus age for paleomagnetic data from (a) Sakhalin, (b) east Sakhalin, and (c) west Sakhalin, with the North American Plate (solid line) and Eurasian Plate (dashed line) as reference APWPs. The range of expected values is indicated for each pole position. Abbreviations for localities are as in Figure 5, with data from *Takeuchi et al.* [1999] indicated by TKO1, TKO2, and TKO3. Sakhalin tectonic events are from *Flecker and Macdonald* [2002]; timing of Japan Sea opening is from *Tamaki et al.* [1992]. Kuril Basin opening is constrained by paleomagnetic data presented here and by *Takeuchi et al.* [1999]. Question marks indicate uncertainty in the dating of tectonic events. Note that in Sakhalin this is particularly important when sediments are paralic because biostratigraphic constraints are potentially subject to large errors.

approximately 400 km south of Dvoynoye River, which suggests that deformation associated with the docking of this relatively small (~10 km scale) terrane is unlikely to have caused the observed rotation at Dvoynoye River. No relative rotation is observed during the Miocene in east Sakhalin. A 25° clockwise-deviated declination observed at Kongi River suggests that the region has rotated clockwise since 8 Ma (Figures 14a and 14b).

[32] If vertical axis rotations are regionally coherent in west Sakhalin (Figure 14c), the data seem to suggest a period of clockwise rotation of up to ~40° from the mid-Paleocene to the late Oligocene. It is most likely that

(a)

(b)

(c)
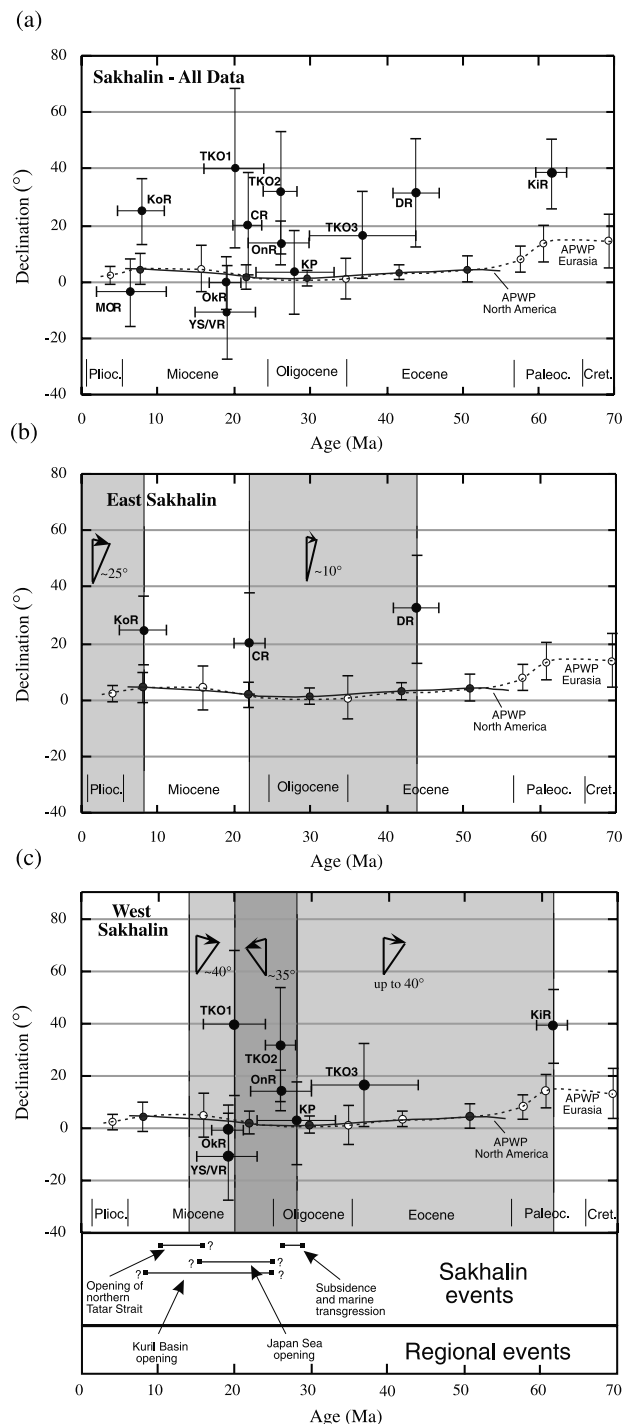
westward directed subduction of the Pacific Plate under Sakhalin in the mid-Paleocene to Eocene [*Bazhenov et al.*, 2001] controlled deformation in both east and west Sakhalin. A terrane docking and indentation event in southern Sakhalin in the Eocene [*Bazhenov et al.*, 2001] may have resulted in a clockwise rigid body rotation at Kitosiya River (mid-Paleocene samples), where paleomagnetic results indicate significantly clockwise deflected declinations (Figure 14). However, the observed vertical axis rotations may also be associated with strike-slip fault deformation, which seems to have begun after the mid-Eocene in east Sakhalin (Figure 14b). Well-documented N-S trending right-lateral strike-slip faults observed in Sakhalin [*Fournier et al.*, 1994] are likely to have accommodated such deformation. Clockwise relative rotation between the late Eocene and the late Oligocene in west Sakhalin (Figure 14c), and clockwise rotation sometime between the middle Eocene and the early Miocene in east Sakhalin (Figure 14b), suggests that a transition from subduction to strike-slip tectonics must have occurred by the late Eocene and that rotational deformation associated with strike-slip faulting affected Sakhalin as a whole. However, with existing data, it is not possible to precisely determine when the vertical axis rotations commenced.

[33] Different characteristics are evident for the Neogene evolution of west Sakhalin compared to east Sakhalin (Figure 14c). Counterclockwise rotation of around 35° appears to have occurred since the Oligocene before a rapid clockwise phase of rotation of about 40° in the early Miocene (~20 Ma). Deformation in southwest Sakhalin, close to the Central Sakhalin Fault, is complex. This is reflected in variable declination values near the Central Sakhalin Fault (Figure 5).

[34] In view of the relatively sparse paleomagnetic data set from Sakhalin, it is difficult to determine to what extent Sakhalin may have deformed as a coherent region and to constrain the significance of deformation at various scales. Further sampling is required in both east and west Sakhalin and close to the central fault. Extensive sampling of well-dated Paleocene-Eocene rocks needs to be carried out to provide precise and independent constraints on the timing of the transition from subduction to strike-slip tectonics in Sakhalin.

5.3. The India-Asia Collision Model

[35] *Jolivet et al.* [1990] and *Worrall et al.* [1996] suggested that the abundance of right-lateral fault systems along the NW Pacific margin was caused by the Eocene collision of India and Asia. This pattern of faulting has been reproduced in analog models, assuming that the eastern edge (the NW Pacific region) is a "free" boundary [*Tapponnier et al.*, 1982; *Peltzer and Tapponnier*, 1988]. The northern boundary of the deformed area in these models is a left-lateral strike-slip fault. *Worrall et al.* [1996] suggested that a continuous fault system links Magadan (northern Okhotsk Sea) westward to Lake Baikal.

[36] There are several problems with this collision-driven model for deformation along the NW Pacific margin. (1) The concept of a "free" boundary clearly does not accurately represent the complex interactions of the Pacific Plate with the North American, Eurasian and/or Okhotsk Sea plates. (2) The age of basins generated by dextral motion along the East Asian margin is not consistent with an India-Asia collision model. In some cases, the basins predate initial collision [*Allen et al.*, 1998]. (3) The case for a linking sinistral fault system from Baikal to Magadan, which would have partially reactivated the Mesozoic Mongol-Okhotsk suture (Figure 1c), is not tenable. In the area to the east of Lake Baikal, the mapped structural grain cross-cuts the trend of the faults required to link to the Mongol-Okhotsk suture; no trace of the postulated linking fault has been found or is apparent in satellite photographs.

[37] Our paleomagnetic data also suggest that the India-Asia collision model is unable to explain observed deformation patterns along the NW Pacific margin. For example, counterclockwise rotations are predicted, based on fault data, in Neogene basins in eastern Sakhalin [*Fournier et al.*, 1994] (Figure 3a). Such rotations would be consistent with deformation generated by extrusion resulting from the India-Asia collision [*Jolivet et al.*, 1994; *Worrall et al.*, 1996]. However, data from the Chamgu, Kongi, and Dvoynoye rivers of east Sakhalin consistently indicate significant clockwise vertical axis rotations (Figure 14b).

5.4. Deformation in Sakhalin Linked to Evolution of the Japan Sea

[38] Initial opening of the Japan Sea has been dated by the $^{40}Ar-^{39}Ar$ technique at between 24 and 17 Ma [*Tamaki et al.*, 1992]. It is frequently assumed that the initial rifting of the Kuril Basin in the Okhotsk Sea (Figure 1a) may have been closely associated with the back-arc opening of the Japan Sea basin and a regional reorganization of interacting continental and oceanic blocks [e.g., *Jolivet and Tamaki*, 1992; *Takeuchi et al.*, 1999]. However, neither the age nor the oceanic nature of the crust in the Kuril Basin has been securely established because it does not exhibit linear seafloor anomalies and has not been drilled.

[39] In southwest Sakhalin, a rapid clockwise vertical axis rotation event (20°–50°), which is significant at the 95% confidence level, can be identified at around 20 Ma (Figure 14c). This is not seen in east Sakhalin (Figure 14b). The timing of this rotation coincides with opening of the Japan Sea (Figure 14c) and probably predates the opening of the Tatar Strait farther to the north near Aleksandrovsk (Figures 1b and 14c) [*Flecker and Macdonald*, 2002]. The observed clockwise rotations in southern Sakhalin might be associated with dextral strike-slip activity on the Central Sakhalin Fault, which continues southward to Hokkaido. In this instance, opening of the Japan Sea Basin would have caused deformation in southern Sakhalin. In some models [*Takeuchi*, 1997; *Takeuchi et al.*, 1999], a mechanism for the observed right-lateral faulting and clockwise rotations in southern Sakhalin is provided by linked opening of the Japan Sea and Kuril Basin followed by southward motion of the Kuril ridge (Figure 3b).

[40] A later phase of 25° of clockwise rotation is observed in east Sakhalin at about 8 Ma (Figure 14b). One possible cause of this may be the cessation of spreading in the Kuril Basin, which would have resulted in increased rates of dextral displacement on N-S trending strike-slip faults along the east coast of Sakhalin and associated clockwise vertical axis rotations of crustal-scale blocks. The declination data can therefore be interpreted to suggest that the Kuril Basin

opened in the Miocene following inferred back-arc opening along an axis parallel to the arc. Spreading in the Kuril Basin, therefore, probably commenced around 24–20 Ma and ceased at about 10–8 Ma (Figure 14c).

5.5. Evidence for the Existence of an Okhotsk Sea Plate

[41] On the basis of earthquake slip data (e.g., the 1995 Neftegorsk earthquake [*Ivashchenko et al.*, 1997], which indicates a transform boundary in northern Sakhalin), *Seno et al.* [1996] suggested that the Okhotsk Sea Plate currently rotates clockwise about a pole in the northern Okhotsk Sea. This gives a solution that takes into account thrust deformation in southern Sakhalin, which the "extrusion" model [*Jolivet et al.*, 1994; *Worrall et al.*, 1996] fails to do. Thus the paleomagnetic data presented here are in agreement with the interpretations of *Seno et al.* [1996], who suggested that the inclusion of an Okhotsk Sea Plate gives a more realistic solution to the geodynamic evolution of the region. Since paleomagnetic data are not available from the Okhotsk Sea Plate, our Sakhalin data are compared with the North American and Eurasian APWPs (Figure 14).

5.6. Style of Deformation in Sakhalin

[42] *Takeuchi et al.* [1999] suggested that domino-style deformation might accommodate clockwise vertical axis rotations inferred from paleomagnetic data from southern Sakhalin (Figure 3b). Their paleomagnetic data are broadly consistent with the new data presented in this study, but they had insufficient data to constrain the details of their domino model (e.g., what happens at the edges of the blocks where they meet the bounding faults?). They also failed to document detailed field evidence for block rotation on either Sakhalin or Hokkaido. Such evidence includes triangular zones of compression and extension that would be expected, where the axes of rotation for the blocks in the deforming zone can be identified [*Roberts*, 1995; *Townsend and Little*, 1998; *Bayasgalan et al.*, 1999]. However, triangular depocenters have been identified from isopach maps of the southern Tatar Strait [*Antipov et al.*, 1980]. *Jolivet et al.* [1994] suggested that these are small pull-apart basins which formed in a similar manner to those documented by *Lallemand and Jolivet* [1986] along the northwestern coast of Honshu, but it is possible that they represent the extensional zones expected to be generated by block rotation.

6. Conclusions

[43] Paleomagnetic inclination data suggest that Sakhalin has remained near its present-day latitude for most of the Tertiary period and that it has evolved with either the Eurasian or the North American plates. Declination data support this interpretation.

[44] Paleomagnetic declination data, when compared with the APWPs for the interacting plates, can be linked to a transition from subduction tectonics to a strike-slip regime in Sakhalin around the middle-late Eocene, but it is not possible to establish the exact timing of the transition. This interpretation is consistent with paleomagnetic data from an exotic terrane, which probably accreted against southeast Sakhalin in the Eocene [*Bazhenov et al.*, 2001]. Different phases of clockwise vertical axis rotation are discernable for

localities in southwest Sakhalin and also in central eastern Sakhalin. A rapid clockwise rotation phase in the early Miocene in southwest Sakhalin may be linked to the onset of rifting in the Japan Sea, Kuril Basin and Tatar Strait. Further rotation in the latest Miocene, which only involved the eastern localities, might be associated with the end of opening in the Kuril Basin and a change of deformation style, with activity on eastern offshore faults near Sakhalin.

[45] Paleomagnetic data are consistent with the block rotation model of *Takeuchi et al.* [1999], but the model remains relatively unconstrained by structural data. Deformation appears to be complex in the southwest and close to the Central Sakhalin Fault, while deformation in eastern areas appears to have been more uniform. Further structural domains may be identified with further sampling.

[46] Our data are in conflict with the model of *Fournier et al.* [1994] which predicted counterclockwise rotations in east Sakhalin due to extrusion at the east Asian margin in response to the India-Asia collision. Clockwise-deflected paleomagnetic declinations agree with a plate reconstruction model proposed by *Seno et al.* [1996], which suggests that the extrusion model is unrealistic and that plate boundary deformation is better described with a separate Okhotsk Sea Plate.

References

Allen, M. B., D. I. M. Macdonald, Z. Xun, S. J. Vincent, and C. Brouet-Menzies, Transtensional deformation in the evolution of the Bohai Basin, northern China, in *Continental Transpressional and Transtensional Tectonics*, edited by R. E. Holdsworth, R. A. Strachan, and J. F. Dewey, *Geol. Soc. Spec. Publ.*, *135*, 215–229, 1998.

Altis, S., Interpretations of a middle Miocene and late Quaternary steady dextral transpression in SW Japan and the opening tectonics for the Japan Sea, *Tectonophysics*, *302*, 257–285, 1999.

Antipov, M. P., V. M. Kovylin, and V. P. Filat'yev, Sedimentary cover of deepwater basins of Tatar Strait and the northern part of the Sea of Japan, *Int. Geol. Rev.*, *22*, 1327–1334, 1980.

Arason, P., and S. Levi, Models of inclination shallowing during sediment compaction, *J. Geophys. Res.*, *95*, 4481–4499, 1990.

Bayasgalan, A., J. Jackson, J.-F. Ritz, and S. Carretier, Field examples of strike-slip fault terminations in Mongolia and their tectonic significance, *Tectonics*, *18*, 394–411, 1999.

Bazhenov, M. L., A. E. Zharov, N. M. Levashova, K. Kodama, N. Y. Bragin, P. I. Fedorov, L. G. Bragina, and S. M. Lyapunov, Paleomagnetism of a Late Cretaceous island arc complex from South Sakhalin, East Asia: Convergent boundaries far away from the Asian continental margin?, *J. Geophys. Res.*, *106*, 19,193–19,205, 2001.

Besse, J., and V. Courtillot, Revised and synthetic apparent polar wander paths of the African, Eurasian, North American and Indian Plates, and true polar wander since 200 Ma, *J. Geophys. Res.*, *96*, 4029–4050, 1991.

Blow, R. A., and N. Hamilton, Effect of compaction on the acquisition of a detrital remanent magnetization in fine-grained sediments, *Geophys. J. R. Astron. Soc.*, *52*, 13–23, 1978.

Fisher, R. A., Dispersion on a sphere, *Proc. R. Soc. London*, *217*, 295–305, 1953.

Flecker, R., and D. I. M. Macdonald, Cenozoic evolution of the Tatar Strait, Russian far east and its relationships to the opening of the Sea of Japan, *Basin Res.*, *217*, in press, 2002.

Fot'yanova, L. M., M. Y. Serova, V. G. Galversen, A. E. Zharov, N. M. Grokhotova, and V. P. Tuzov, Key section of the Paleogene deposits of the Kril'on Peninsula (south Sakhalin, Kitosiya River) (in Russian), *Strat. Geol. Correl.*, *9*, 58–76, 2001.

Fournier, M., L. Jolivet, P. Huchon, K. F. Sergeyev, and L. S. Oscorbin, Neogene strike-slip faulting in Sakhalin and the Japan Sea opening, *J. Geophys. Res.*, *99*, 2701–2725, 1994.

Fuller, M., R. Haston, and E. Schmidtke, Paleomagnetism in SE Asia: Sinistral shear between Philippine Sea plate and Asia, in *Paleomagnetic Rotations and Continental Deformation*, *NATO Sci. Ser., Ser. C*, vol. 254, edited by C. Kissel and C. Laj, pp. 411–430, Kluwer Acad., Norwell, Mass., 1989.

Gladenkov, Y. B., Neogene stratigraphy of northeast Asia (Kamchatka, Sakhalin, in *Pacific Neogene Datum Planes*, edited by N. Ikebe and R. Tsuchi, pp. 235–243, Univ. of Tokyo Press, Tokyo, 1988.

Gordon, R. G., and R. Van der Voo, Mean paleomagnetic poles for the major continents and the Pacific Plate, in *A Handbook of Geophysical Constants*, *AGU Ref. Shelf*, vol. 1, edited by T. J. Ahrens, pp. 225–239, AGU, Washington, D. C., 1995.

Hodych, J. P., and S. Bijaksana, Can remanence anisotropy detect paleomagnetic inclination shallowing due to compaction?, *J. Geophys. Res.*, *98*, 22,429–22,441, 1993.

Hodych, J. P., and K. L. Buchan, Early Silurian palaeolatitude of the Springdale Group redbeds of central Newfoundland: A palaeomagnetic determination with a remanence anisotropy test for inclination error, *Geophys. J. Int.*, *117*, 640–652, 1994.

Hodych, J. P., S. Bijaksana, and R. Patzold, Using magnetic anisotropy to correct for paleomagnetic inclination shallowing in some magnetite-bearing deep-sea turbidites and limestones, *Tectonophysics*, *307*, 191–205, 1999.

Hornafius, J. S., B. P. Luyendyk, R. R. Terres, and M. J. Kamerling, Timing and extent of Neogene tectonic rotation in the western Transverse Ranges, California, *Geol. Soc. Am. Bull.*, *97*, 1476–1487, 1986.

Ivashchenko, A. I., C. U. Kim, L. S. Oscorbin, L. N. Poplavskaya, A. A. Poplavskiy, R. N. Burymskaya, T. G. Mikhailova, N. F. Vasilenko, and M. I. Streltsov, The Neftegorsk, Sakhalin Island, earthquake of 27 May 1995, *Island Arc*, *6*, 288–302, 1997.

Jackson, J. A., and P. Molnar, Active faulting and block rotations in the western Transverse Ranges, California, *J. Geophys. Res.*, *95*, 22,073–22,087, 1990.

Jackson, M., W. Gruber, J. Marvin, and S. K. Banerjee, Partial anhysteretic remanence and its anisotropy: Applications and grainsize-dependence, *Geophys. Res. Lett.*, *15*, 440–443, 1988.

Jackson, M. J., S. K. Banerjee, J. A. Marvin, R. Lu, and W. Gruber, Detrital remanence, inclination errors, and anhysteretic remanence anisotropy: Quantitative model and experimental results, *J. Geophys. Int.*, *104*, 95–103, 1991.

Jolivet, L., and K. Tamaki, Neogene kinematics in the Japan Sea region and volcanic activity of the northeast Japan arc, *Proc. Ocean Drill. Program Sci. Results*, *127–128*, 1311–1331, 1992.

Jolivet, L., P. Davy, and P. Cobbold, Right-lateral shear along the northwest Pacific margin and the India-Eurasia collision, *Tectonics*, *9*, 1409–1419, 1990.

Jolivet, L., K. Tamaki, and M. Fournier, Japan Sea, opening history and mechanism: A synthesis, *J. Geophys. Res.*, *99*, 22,237–22,259, 1994.

Jolivet, L., H. Shibuya, and M. Fournier, Paleomagnetic rotations and the Japan Sea opening, in *Active Margins and Marginal Basins of the Western Pacific*, *Geophys. Monogr. Ser.*, vol. 88, edited by B. Taylor and J. Natland, pp. 355–369, AGU, Washington, D. C., 1995.

Kharakhinov, V. V., S. D. Gal'tsev-Bezyuk, and A. A. Tereshchenkov, Faults of Sakhalin, *Geol. Pac. Ocean*, *3*, 355–373, 1985.

Kimura, G., The latest Cretaceous-early Paleogene rapid growth of accretionary complex and exhumation of high pressure series metamorphic rocks in northwestern Pacific margin, *J. Geophys. Res.*, *99*, 22,147–22,164, 1994.

Kirschvink, J. L., The least-squares line and plane and the analysis of palaeomagnetic data, *Geophys. J. R. Astron. Soc.*, *62*, 699–718, 1980.

Kissel, C., and C. Laj, The Tertiary geodynamic evolution of the Aegean arc: A paleomagnetic reconstruction, *Tectonophysics*, *146*, 183–201, 1988.

Kodama, K. P., A successful rock magnetic technique for correcting paleomagnetic inclination shallowing: Case study of the Nacimiento Formation, New Mexico, *J. Geophys. Res.*, *102*, 5193–5205, 1997.

Lallemand, S., and L. Jolivet, Japan Sea-A pull-apart basin, *Earth Planet. Sci. Lett.*, *76*, 375–389, 1986.

Little, T. A., and A. P. Roberts, Distribution and mechanism of Neogene to present-day vertical axis rotations, Pacific-Australian plate boundary zone, South Island, New Zealand, *J. Geophys. Res.*, *102*, 20,447–20,468, 1997.

Luyendyk, B. P., M. J. Kamerling, and R. R. Terres, Geometric model for Neogene crustal rotations in southern California, *Geol. Soc. Am. Bull.*, *91*, 211–217, 1980.

Luyendyk, B. P., M. J. Kamerling, R. R. Terres, and J. S. Hornafius, Simple shear of Southern California during Neogene time suggested by paleomagnetic declinations, *J. Geophys. Res.*, *90*, 12,454–12,466, 1985.

Menner, V. V., Y. P. Baranova, and L. S. Zhidkova, Neogene of the northeastern USSR (Kolyma Region, Kamchatka and Sakhalin), in *Proceedings of the First International Congress of Pacific Neogene Stratigraphy*, edited by T. Saito and H. Ujiie, pp. 82–88, Tokyo, 1977.

Natal'in, B., History and modes of Mesozoic accretion in southeastern Russia, *Island Arc*, *2*, 15–34, 1993.

Nur, A., H. Ron, and O. Scotti, Mechanics of distributed fault and block rotation, in *Paleomagnetic Rotations and Continental Deformation*, *NATO Sci. Ser., Ser. C*, vol. 254, edited by C. Kissel and C. Laj, pp. 209–228, Kluwer Acad., Norwell, Mass., 1989.

Okamura, S., Y. A. Martynov, K. Furuyama, and K. Nagao, K-Ar ages of the basaltic rocks from far east Russia: Constraints on the tectono-magmatism associated with the Japan Sea opening, *Island Arc*, *7*, 271–282, 1998.

Otofuji, Y., T. Itaya, and T. Matsuda, Rapid rotation of southwest Japan—Palaeomagnetism and K-Ar ages of Miocene volcanic rocks of southwest Japan, *Geophys. J. Int.*, *105*, 397–405, 1991.

Parfenov, L. M., and B. A. Natal'in, Mesozoic tectonic evolution of northeastern Asia, *Tectonophysics*, *127*, 291–304, 1986.

Peltzer, G., and P. Tapponnier, Formation and evolution of strike-slip faults, rifts, and basins during the India-Asia collision: An experimental approach, *J. Geophys. Res.*, *93*, 15,085–15,117, 1988.

Riegel, S. A., K. Fujita, B. M. Koz'min, V. S. Imaev, and D. B. Cook, Extrusion tectonics of the Okhotsk Plate, northeast Asia, *Geophys. Res. Lett.*, *20*, 607–610, 1993.

Rikhter, A. V., The structure, age and structural setting of the metamorphic rocks of Sakhalin (in Russian), *Geotektonica*, *6*, 55–65, 1984.

Roberts, A. P., Tectonic rotation about the termination of a major strike-slip fault, Marlborough fault system, New Zealand, *Geophys. Res. Lett.*, *22*, 187–190, 1995.

Rozhdestvenskiy, V. S., The role of wrench-faults in the structure of Sakhalin, *Geotectonics*, *16*, 323–332, 1982.

Seno, T., T. Sakurai, and S. Stein, Can the Okhotsk plate be distinguished from the North American plate?, *J. Geophys. Res.*, *101*, 11,305–11,315, 1996.

Serova, M. Y., and L. M. Fot'yanova, Paleogene-Neogene boundary in heterofacieal deposits of Sakhalin and Kamchatka, in *Monographic Proceedings of IGCP-114 International Workshop on Pacific Neogene Biostratigraphy*, edited by N. Ikebe, pp. 135–136, Int. Geol. Correlation Programme, Paris, 1981.

Takeuchi, T., K-Ar ages of the Tertiary volcanic rocks in South Sakhalin and their tectonic significance (in Japanese), *J. Geol. Soc. Jpn.*, *103*, 67–79, 1997.

Takeuchi, T., K. Kodama, and T. Ozawa, Paleomagnetic evidence for block rotations in central Hokkaido-south Sakhalin, northeast Asia, *Earth Planet. Sci. Lett.*, *169*, 7–21, 1999.

Tamaki, K., K. Suyehiro, J. Allan, J. C. Ingle, and K. Pisciotto, Tectonic synthesis and implications of Japan Sea ODP drilling, *Proc. Ocean Drill. Program Sci. Results*, *127–128*, 1333–1350, 1992.

Tan, X., and K. P. Kodama, Compaction-corrected inclinations from southern California Cretaceous marine sedimentary rocks indicate no paleolatitudinal offset for the Peninsular Ranges terrane, *J. Geophys. Res.*, *103*, 27,169–27,192, 1998.

Tapponnier, P., G. Peltzer, A. Y. Le Dain, R. Armijo, and P. Cobbold, Propagating extrusion tectonics in Asia: New insights from simple experiments with plasticine, *Geology*, *10*, 611–616, 1982.

Tauxe, L., and G. Watson, The fold test: An eigen analysis approach, *Earth Planet. Sci. Lett.*, *122*, 331–341, 1994.

Tauxe, L., C. G. Constable, L. Stokking, and C. Badgley, Use of anisotropy to determine the origin of characteristic remanence in the Siwalik red beds of northern Pakistan, *J. Geophys. Res.*, *95*, 4391–4404, 1990.

Tauxe, L., N. Kylstra, and C. Constable, Bootstrap statistics for paleomagnetic data, *J. Geophys. Res.*, *96*, 11,723–11,740, 1991.

Townsend, D. B., and T. A. Little, Pliocene-Quaternary deformation and mechanisms of near-surface strain close to the eastern tip of the Clarence Fault, northeast Marlborough, *N. Z. J. Geol. Geophys.*, *41*, 401–417, 1998.

Vereshchagin, V. N., Geological map of Sakhalin, Minist. of Geol. of the USSR, Moscow, 1969.

Watson, G. S., A test for randomness, *Mon. Not. R. Astron. Soc.*, *7*, 160–161, 1956.

Weaver, R., A. P. Roberts, and A. J. Barker, A late diagenetic (synfolding) magnetization carried by pyrrhotite: Implications for paleomagnetic studies from magnetic iron sulphide-bearing sediments, *Earth Planet. Sci. Lett.*, *200*, 371–386, 2002.

Worrall, D. M., V. Krugliak, F. Kunst, and V. Kuznetsov, Tertiary tectonics of the Sea of Okhotsk, Russia: Far-field effects of the India-Eurasia collision, *Tectonics*, *15*, 813–826, 1996.

Zhidkova, L. S., and B. A. Sal'nikov, Reference section of Paleogene-Neogene deposits of south-east Sakhalin (Makarov section), VNIGRI, St. Petersburg, 1992.

Zonenshain, L. P., M. I. Kuz'min, and L. V. Natapov, *Geology of the USSR: A Plate Tectonic Synthesis*, *Geodyn. Ser.*, vol. 21, 242 pp., AGU, Washington D. C., 1990.

Zyabrev, V. S., and N. Y. Bragin, Deep water terrigenous sedimentation in the West Sakhalin Trough, *Dokl. Akad. Nauk SSSR*, *292*, 168–171, 1987.

————————————

R. Flecker, School of Geographical Sciences, University of Bristol, University Road, Bristol BS8 1SS, UK.

L. M. Fot'yanova, Paleontological Institute, Russian Academy of Sciences, 109017 Moscow, Russia.

D. I. M. Macdonald, Department of Geology and Petroleum Geology, University of Aberdeen, Meston Building, Aberdeen AB24 3UE, UK.

A. P. Roberts and R. Weaver, School of Ocean and Earth Science, University of Southampton, Southampton Oceanography Centre, Southampton SO14 3ZH, UK. (rweaver@mail.soc.soton.ac.uk)